



HAL
open science

On the modeling of electric railway lines for the assessment of infrastructure impact in radiated emission tests of rolling stock

Andrea Cozza, Bernard Demoulin

► **To cite this version:**

Andrea Cozza, Bernard Demoulin. On the modeling of electric railway lines for the assessment of infrastructure impact in radiated emission tests of rolling stock. *IEEE Transactions on Electromagnetic Compatibility*, 2008, 50 (3), pp.566-576. 10.1109/TEM.2008.924387 . hal-00352186

HAL Id: hal-00352186

<https://centralesupelec.hal.science/hal-00352186>

Submitted on 17 Nov 2010

HAL is a multi-disciplinary open access archive for the deposit and dissemination of scientific research documents, whether they are published or not. The documents may come from teaching and research institutions in France or abroad, or from public or private research centers.

L'archive ouverte pluridisciplinaire **HAL**, est destinée au dépôt et à la diffusion de documents scientifiques de niveau recherche, publiés ou non, émanant des établissements d'enseignement et de recherche français ou étrangers, des laboratoires publics ou privés.

On the Modeling of Electric Railway Lines for the Assessment of Infrastructure Impact in Radiated Emission Tests of Rolling Stock

Andrea Cozza, *Member, IEEE*, and Bernard Démoulin

Abstract—In this paper, we address the problem of testing radiated emissions generated by rolling stock, when carried out on actual railway sites, as prescribed by the standard EN 50121. The idea of assessing infrastructure impact on test results is presented here by means of an electromagnetic model of railway sites. In the first part, modeling tools are introduced together with some results from the experimental validation. These tools are then applied to actual railway lines proving the importance of site resonances and the ambiguities in the application of the standard EN 50121 in the industrial domain. After pointing out the main difficulties in the simulation of actual railway sites, we present a feasibility study of an alternative procedure for the modeling of a site, based on magnetic field measurements and the solution of an inverse problem with no *a priori* information about the test site configuration.

Index Terms—Electromagnetic (EM) radiation, inverse problems, multiconductor transmission lines, standards, transportation.

I. PROBLEM DESCRIPTION AND INDUSTRIAL BACKGROUND

THE DRAMATIC increase in the use of electronic devices in almost any domain has led to a substantial rise of the potential for interference between equipment working in the same environment. Because of the likely disruptions that may follow this scenario, electromagnetic compatibility (EMC) has established itself as the cornerstone for the proper working of any electronic equipment.

The railway domain has been part of this trend since the early introduction of static conversion through power transistors acting as switches, through switched-mode conversion/regulation, that generates strong current/voltage gradients leading to interference phenomena that could jeopardize the proper working of electronic devices within the train itself and the correct interpretation of railway control signals propagating along the rails. This is a major issue because of the inherent security hazards involved: the failing of security and control devices could have dire consequences. This was a major point for the introduction of EMC testing of rolling stock. Moreover, electromagnetic in-

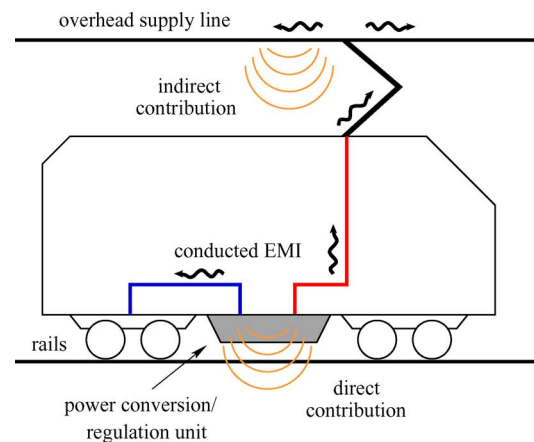


Fig. 1. Schematic representation showing the main interference phenomena generated by the switched-mode conversion unit onboard an electric train.

terference (EMI) can affect, through radiation and propagation, other systems not directly related to the railway domain, such as telecommunications lines and wireless systems [1]. Typical maximum levels of the magnetic field imposed by the standard are of the order of $45 \text{ dB} \cdot \mu\text{A}/\text{m}$ at 100 kHz, as measured by a 200-Hz bandwidth receiver [2]. The actual masks imposed depend on the frequency as well as on the railway infrastructure and technology.

The main phenomena involved in the EMC of electric trains can be broadly summarized through the paradigm introduced in Fig. 1, depicting a train supplied by an overhead line. The absorbed electrical energy is converted and/or regulated by a switched-mode unit, in order to ensure all the different electrical energy supplies required for its functioning. The inherently strong current and voltage time derivatives generate conducted EMI that propagate along the internal cabling: part of them will affect other devices inside the train itself, whereas another part will reach the train pantograph and then the supply line, thus affecting the world outside the train. On the other hand, the switched-mode unit will also directly excite an electromagnetic (EM) field outside the train, thus giving place to radiated EMI. Nevertheless, these are not the only effects caused by EMI generated by the train: as a matter of fact, the current injected into the supply line (overhead wires, rails, ground wires), and propagating along it, is bound to give an indirect contribution to the overall EM field excited by the train. Therefore, it is no wonder that EMC standards have been introduced, dealing with the generation of EMI. Their main aim is to set maximum levels

Manuscript received June 18, 2007; revised December 21, 2007.

A. Cozza is with the Electromagnetics Research Department, L'École Supérieure d'Électricité (SUPELEC), 91192 Gif-sur-Yvette, France (e-mail: andrea.cozza@supelec.fr).

B. Démoulin is with the Telecommunication, Interferences and Electromagnetic Compatibility (TELICE), Institut d'Électronique, de Microélectronique et de Nanotechnologie (IEMN) Laboratory, Université de Sciences et Technologies de Lille, 59655 Villeneuve d'Ascq Cedex, France (e-mail: bernard.demoulin@univ-lille1.fr).

Color versions of one or more of the figures in this paper are available online at <http://ieeexplore.ieee.org>.

Digital Object Identifier 10.1109/TEMC.2008.924387

for conducted and radiated EMI generated by rolling stock and power supply substations. In the context of the European Union, the reference in railway EMC is set by the European Committee for Electrotechnical Standardization (CENELEC) standard EN 50121 [2].

The introduction of this standard in 1996 in its experimental version, later updated in 2000, has proven to be a formidable drive toward a stronger commitment to EMC on the manufacturer side. Since trains cannot be tested in standard facilities such as anechoic chambers due to practical problems (dimensions, power supply, etc.), the only practical way of performing these tests is to consider actual railway lines, where the train can be operated more easily.

Actual configurations of railway lines vary, both geometrically, and topologically and electrically [3], [4]: while these differences are not expected to affect the generation of EMI from the train itself [5], which can be indeed regarded as an independent EMI source, they are expected to have by far a greater impact on the indirect contribution to radiated EMI. Therefore, the overall EM field measured near a train would depend in part on the test site configuration. This problem is worsened by the likely excitation of resonances along the supply line, due to low propagation attenuation (see Section III). The excitation of undamped resonances would ultimately lead to sharp maxima in radiated EMI. While dealing with a standard, tests should yield comparable results whatever railway structure they are carried out on. The solution envisaged by the CENELEC committee was to perform the tests related to the train on a line ideally infinitely long, clear of any electrical discontinuities along it, since such a configuration would be the simplest and least ambiguous one to be considered. This is due to the fact that along an infinite uniform line, no reflection can occur, hence no resonances. Although actual sites never fulfill such requirements, they can acceptably approximate them as long as reflections coming back toward the train are negligible, a condition that is met whenever the propagation attenuation is strong enough, i.e., for a lossy line long enough to have reflections reduced to negligible levels. To this end, the CENELEC committee prepared a set of guidelines to be followed in order to minimize the infrastructure impact [2], following the basic idea of obtaining results reproducible on other test sites. In particular, the concept of a minimum length of the test track was introduced.

Considering this scenario, it appears quite obvious why, amid other tests, characterizing radiated emissions near a train is considered a critical task. Whenever the line resonates at a given frequency where the train generates important conducted EMI, relatively strong EM field maxima occur; unfortunately, it is very difficult to decide whether a maximum has been actually “amplified” by the infrastructure or not. This also explains why the customer always requires the manufacturer to perform the tests on his own site, i.e., in order to be sure that the train is standard-compliant on the site where the train will be used, rather than on a generic facility. The standard acknowledges this problem, suggesting an ambient noise characterization by measuring the EM field radiated by the supply line while the train is not yet present. The underlying idea is to exploit the conducted EMI generated by power supply substations as a mean to high-

light the presence of resonances. Eventually, the comparison of the ambient noise spectrum with the actual test results would justify strong peaks in the spectrum measured near the train as due to line resonances. Nevertheless, this would not yield any quantitative information on the infrastructure impact.

This problem is a major issue for the manufacturer, since it can prove to be a tough job to demonstrate to the customer that the excessive radiation of a train is partly due to the test site. Moreover, the guidelines given by the standard cannot always be satisfied, thus increasing the odds of exceeding the standard-imposed limits. Such an outcome can have important repercussions on the manufacturer: delays in the delivery schedule, extra costs in order to reduce seemingly excessive EMI, and so on. These considerations have led Alstom Transport, a rolling stock manufacturer, and the Centre d'Essai Ferroviaire (CEF), a railway test facility, to propose a research project addressing these issues [6]. The aim was to study the phenomena involved in the generation of the EM field near a train, in order to develop a theoretical model for the assessment of the infrastructure impact on test results, by simulating radiated EMI tests along actual test sites and an ideal infinite one, i.e., closed on matched loads. Such a tool could be used as a qualitative and quantitative way of proving to a customer that excessive levels in the measured EM field spectra may be due to the site infrastructure rather than due to the train. This would allow the manufacturer to argue on the consistency of the test methods and results, showing that not all the blame can be put on to him. To this end, this tool should be as simple as possible, while giving sound results. As a matter of fact, it would not be practical to use full-wave simulators due to the sheer dimensions of a railway site; this would require hours of computations, whereas the customer usually allows the manufacturer inside his site only for a very limited amount of time. Furthermore, not even the customer has a detailed description of the actual configuration of his site, so that the model to be used is bound to be an extremely simplified one: this problem is addressed in Section III.

This paper is organized as follows. In Section II, we present the theoretical tools that have been employed for the modeling of uniform railway lines; the difficulties in modeling actual lines are then addressed in Section III, whereas experimental results validating the model are presented in Section IV. Finally, we show how these tools can be utilized for the assessment of the infrastructure impact: first in a predictive way, given a sufficiently detailed equivalent description of the railway site, and then, in an alternative way, based on an experimental characterization of the site, with no *a priori* information.

II. MODELING TOOLS FOR A RAILWAY LINE

Industrial experience within Alstom Transport has shown that resonances pose problems mainly below 1 MHz. The standard EN 50121 only requires the measurement of the y -component H_y (Fig. 2) of the magnetic field up to 30 MHz at a distance of 10 m away from the track axis, with the mechanical center of the loop antenna 1–2 m high above the soil, facing the train under test (TUT). Therefore, our investigations were limited just to H_y up to about 1–2 MHz, by means of near-field antenna

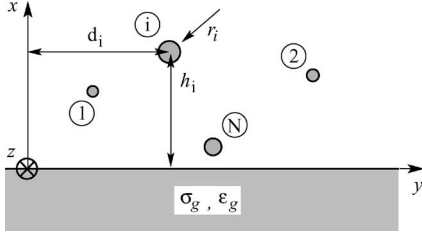


Fig. 2. Railway line as a transmission line structure: cross section.

theory models. Actually, the TUT is to be tested under two basic configurations: a static (no traction devices activated) and a slow motion one. A static configuration will be assumed hereafter; nevertheless, the results obtained in this way can still be used for the slow-motion configuration.

An effective and simple tool for the modeling of line structures is transmission line theory (TLT), based on a quasi-TEM approximation. A good adherence to experimental results is expected as long as each conductor is electrically near to the ground–plane interface. This assumption holds for the typical values h_i encountered in railway lines, over the frequency ranges that we are interested in here. Attention should be given to the fact that soil cannot be approximated as a perfect conductor: in this paper, it will be assumed to be a homogeneous half-space characterized by a complex relative dielectric constant $\tilde{\epsilon} = \epsilon_g - j\sigma_g/(\omega\epsilon_0)$, with $\epsilon_g \in [5, 15]$ and $\sigma_g \in [1, 100]$ mS/m [7]. A typical value is $\sigma_g = 10$ mS/m. A sensitivity analysis [6] has pointed out that ϵ_g has a negligible effect on the overall system behavior, since the soil transition from lossy conductor to lossy dielectric, i.e., $\sigma_g = \omega\epsilon_0\epsilon_g$, occurs above 2 MHz, even for a low-conductivity soil (sandy soils, 1 mS/m). The consequences of a finitely conducting ground–plane have been investigated in many works over the past century; concerning TLT, the validity of the quasi-TEM approximation has been investigated in [8] and [9] from a theoretical point of view and experimentally in [10], showing that the quasi-TEM mode still dominates for conductors electrically close to the soil interface.

Propagation is simply described once per-unit-length parameters (PULP) are known. Simple closed-form expressions are available for an MTL above a lossless ground–plane [11]; nevertheless, the finite soil conductivity modifies these parameters. It was first shown in [12] that the computation of PULP for a lossy soil can be addressed by decomposing it into two parts: the first one corresponds to the external PULP \mathbf{Z}_e , \mathbf{Y}_e , computed by regarding the soil as a perfect conductor, whereas the second part \mathbf{Z}_g , \mathbf{Y}_g accounts for the soil finite conductivity, as

$$\mathbf{Z} = \mathbf{Z}_e + \mathbf{Z}_g \quad (1a)$$

$$\mathbf{Y}^{-1} = \mathbf{Y}_e^{-1} + \mathbf{Y}_g^{-1}. \quad (1b)$$

The closed-form expressions reported in Appendix A have been used, as derived in [13] from the theoretical model proposed in [14]. Those results have been obtained under a thin-wire approximation, which is usually invoked whenever $h/r \gg 1$; although this condition is not satisfied by rails, it has been proven [15] that the actual condition to satisfy is $h_i/r_i > 1$, i.e., for conductors almost in contact with the soil interface. This

condition is actually met by rails too; moreover, the analysis of a railway line can be further simplified by considering equivalent circular rails rather than their actual profile. This would allow the use of all the formulas in Appendix A without any need to employ numerical methods for the computation of the PULP. The estimation of the equivalent rail radius has been carried out in [6]: actual rail profiles were approximated as a bundle of equipotential thin-wire conductors, while computing the overall PULP of the entire rail as suggested in [11]. Subsequently, the thin-wire formulas in Appendix A have been applied, computing the equivalent radius that would be necessary in order to have the same PULP as for the actual rail. This radius was found to be equal to 76 mm for a standard UIC60 rail; with a typical height above the soil around 30–60 cm, rails largely satisfy the thin-wire approximation.

Once the PULP of the MTL are known, voltages and currents can be computed easily by means of the following expressions:

$$\mathbf{V}(z) = \mathbf{Z}_c \mathbf{T} [\mathbf{P}^+(z) \mathbf{I}_{m0}^+ + \mathbf{P}^-(z) \mathbf{I}_{m0}^-] \quad (2a)$$

$$\mathbf{I}(z) = \mathbf{T} [\mathbf{P}^+(z) \mathbf{I}_{m0}^+ - \mathbf{P}^-(z) \mathbf{I}_{m0}^-] \quad (2b)$$

where $\mathbf{P}^\pm(z) = \exp(\mp\gamma z)$ are the propagation matrices, \mathbf{Z}_c is the characteristic impedance matrix, γ is the diagonal matrix of modal propagation constants, and \mathbf{I}_{m0}^\pm are modal current excitation terms depending on boundary conditions at the line ends. Matrix \mathbf{T} and the propagation constants are related to the PULP matrices by means of the following eigenvalue expression:

$$(\mathbf{Y}\mathbf{Z})\mathbf{T} = \mathbf{T}\gamma^2. \quad (3)$$

A major issue in the analysis of railway systems is the modeling of power devices such as power supply substations, trains, overvoltage protections, and so on. Because these devices are electrically small, up to a few megahertz, they can all be modeled as lumped discontinuities. Although simplified equivalent circuits are available up to a few kilohertz for electric trains, characterizations covering an extended frequency range are not easily available. The reason for this lack of data is not only the fact that trains are tailor-made according to the customer's needs, but also due to practical difficulties in the experimental characterization of an active device that needs to be supplied under several thousands volts. Since this problem is common to any effort concerning railway systems modeling, this topic will not be addressed; this paper focuses on the way available models can be employed for the assessment of infrastructure impact.

Once equivalent representations are available for MTLs and lumped discontinuities, a railway system can be represented by means of an equivalent circuit that can be solved with well-established electric network analysis tools, e.g., the tableau method. In particular, the quantities we are interested in are the modal terms \mathbf{I}_{m0}^\pm for the line in front of the observer. Having access to their values, the current distribution along each conductor of this line can be computed by means of (2b).

The EM field radiated by a railway line can now be computed by means of antenna-theory methods. Wait's model [14], already used for the derivation of the PULP, can be applied, thus taking into account soil losses. The application of this model is very convenient, since it directly links the EM field in any point of the

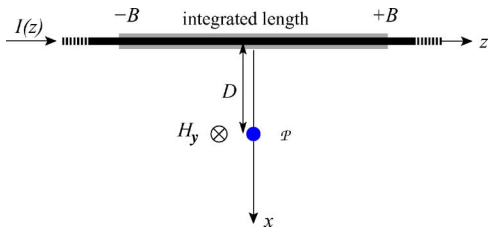


Fig. 3. Simplified configuration considered in order to check the accuracy of the magnetic field computed with finite integration bounds for an infinite line.

space with the current distribution. In its original formulation, the line was regarded as a single conductor. An extension to an MTL was proposed in [16], exploiting the modal decomposition applied in (2b). The magnetic field at position (x_o, y_o, z_o) can be computed as

$$H_y(x_o, y_o, z_o) = \sum_{i=1}^N \sum_{j=1}^N \Theta_{ik}(x_o, y_o) T_{ik} I_{m,k}(z_o) \quad (4)$$

where the current distribution $I_{m,k}(z)$ along the k th modal line is defined as

$$I_{m,k}(z) = I_{m0,k}^+ e^{-\gamma_k z} - I_{m0,k}^- e^{+\gamma_k z} \quad (5)$$

while the radiation matrix $\Theta(x, y)$ is given in Appendix B. The computation of the radiation matrix is relatively time-consuming because of the necessity to evaluate Sommerfeld integrals. A logarithmic approximation [17] can be applied to one of these integrals, yielding an analytical solution; for the remaining ones, rather than numerically integrating them, their kernel was approximated through Prony's method [18]. The result of this operation is the expansion of the kernels of Sommerfeld integrals into a complex exponential sum, such as

$$f(\lambda) \simeq \sum_{i=1}^N c_i e^{a_i \lambda} \quad (6)$$

which can be easily integrated analytically. The expansion parameters c_i and a_i are obtained through a nonlinear fitting procedure.

The only problem with Wait's model is that it assumes the line to be infinitely long. Since this is never the case, one must check when and how this model can be applied to finite lines. Let us consider an infinite line: one could rightfully claim that the main contribution to the magnetic field comes from a portion $2B$ of line centered just in front of the observer. In other words, there exists a B so that the contribution from the portion $[-\infty, -B] \cup [B, +\infty]$ is negligible; under such conditions, an infinite line behaves as if it were finite for the radiation estimate.

In order to check under which conditions this approximation can be invoked, let us consider a complex exponential current distribution in free space along the z -axis, as in Fig. 3. The magnetic field it excites can be computed by convolving the current distribution with the free-space Green's function; the absolute value of the resulting integrand function is mainly proportional to the function $1/\rho^3$ in the near-field. The error introduced by

this approximation is actually negligible, since the observer is in the very near-field of the radiator ($D \leq 10$ m, $f < 1$ MHz); this corresponds to a quasi-static configuration, even though a complex current distribution has been considered. For such a simple configuration, one can analytically compute the magnetic field at a distance D from the line (see Fig. 3), as excited by the entire infinite current distribution; in the same way, one can compute the contribution given by a limited portion of the current distribution, over a range $z \in [-B, +B]$. The definition of the integration efficiency η as in (7) allows us to assess the accuracy that can be attained by fixing a bound B

$$\eta[1/\rho^3] = \frac{\int_{-B}^{+B} dz/\rho^3}{\int_{-\infty}^{+\infty} dz/\rho^3} = \frac{B/D}{\sqrt{1 + (B/D)^2}}. \quad (7)$$

Although derived under strong approximations, expression (7) works remarkably well. By fixing an accuracy $\eta > 0.9$ (error < 1 dB), one gets $B/D > 3$; this rule of thumb has been checked by computing the magnetic field along an MTL through the numerical integration of Sommerfeld's model for an electric dipole above a lossy soil [19], limiting the integration to the interval $[-B, +B]$ given by (7) and comparing these results to Wait's infinite line model. The cross section of the line has been chosen to represent an actual railway line, with a length of 1 km: the results obtained just below the overhead conductors and 10 m away from them have proven that (7) is actually slightly conservative [6].

Practically, this rule of thumb means that an infinite line model can be applied to a finite one as long as the observer is at a distance B from any discontinuities. This also implies that the modeling tools presented here cannot be used for the computation of the magnetic field as measured in front of a train. This limitation is not only due to the use of an infinite line model, but also due to the fact that the presence of the train chassis would inevitably require a numerical approach. Nevertheless, this is not a limitation with respect to the target set here: even though the magnetic field is measured away from the train position, the tools introduced here can be effectively used for the estimation of the infrastructure impact. Actually, (7) yields $B > 30$ m for an observer 10 m away from the line: this distance is electrically small up to 1 MHz, so that the magnetic field is not expected to vary appreciably along it.

III. ON THE MODELING OF ACTUAL LINES

Before applying the modeling tools presented in Section II to actual railway lines, there are still some open issues. The paradigm of a uniform MTL introduced in the previous section can be regarded, at first, as not really fit to model a railway line (Fig. 4); the main points that could be raised are the presence of: 1) discontinuities provided by masts; 2) a rock ballast below the rails; and 3) short circuits between the overhead conductors.

The problem with the first point is that, should the masts have a nonnegligible effect, one would need to include them in the railway system description, by means of lumped circuits, every 50–70 m, thus increasing the system complexity. Numerical simulations of realistic mast structures using numerical electromagnetics code 2 (NEC2) (method of moments) have shown

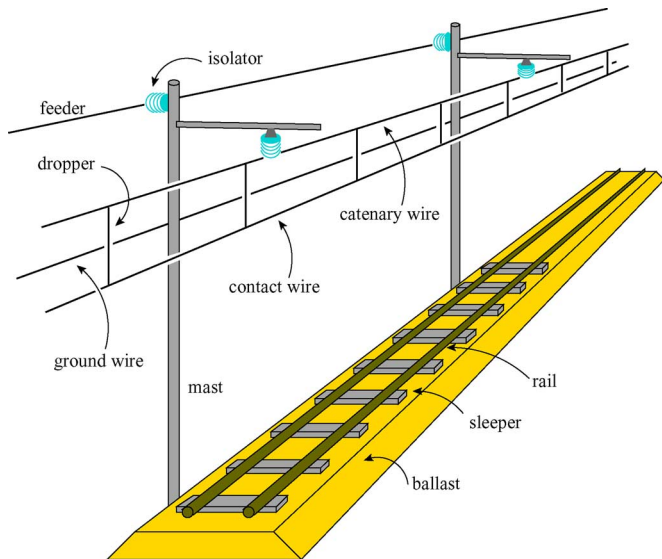


Fig. 4. Schematic representation of an actual railway line.

that they can be effectively modeled as $13\text{-}\mu\text{H}$ inductances up to 3 MHz [6]. Nevertheless, masts are always connected in series to overhead conductors by means of power isolators: since these latter ones basically behave as capacitances limited to a few picofarads, they dominate the overall impedance seen from the railway line, providing a very high impedance path. Simulations including masts and power isolators have shown no remarkable differences in the current distribution with respect to the case of a uniform structure, so that the presence of masts can be neglected.

Another point is the presence of a rock ballast. Other authors [20], [21] have presented results from the experimental estimation of the PULP of a railway line, showing that a rock ballast introduces equivalent conductances between the rails and the soil. Nevertheless, the effect of the rock ballast is expected to be mostly negligible over the frequency range investigated here; the argument that can be brought to this claim is that rock ballasts are made of low conductive rocks (mostly quartzite), which are not electrically connected, but rather interfilled with air. Usually this argument is regarded as insufficient due to the high humidity rates that can be attained during rainy weather. Nevertheless, the experimental results shown in Section IV have been obtained exactly with such conditions, thus suggesting the validity of this approximation.

The last argument is the presence of short circuits along the overhead conductors. The electrical distance between them is short enough to apply the idea of having distributed short circuits along the overhead conductors, rather than lumped ones. The advantage of this approach is that we can directly intervene on the PULP representation of the MTL; considering all the overhead conductors as equipotential implies that the catenary system inherently behaves as a single conductor. Equivalent PULP can then be derived for this equivalent representation [11] with just one equivalent overhead conductor. The resulting reduction in the catenary complexity implies a reduction of the computation time spent in solving the equivalent railway circuit and in the

computation of the radiation matrix Θ . With respect to this last point, the equivalent overhead conductor lays in the mechanical center of the original overhead bundle. The idea of an equivalent single-wire catenary also provides an easy way to check the importance of nonuniformities in the overhead line, namely a camber. Its importance can be assessed by computing the equivalent PULP for the cross section in the two extreme positions of the camber of a real-life line: a three-wire overhead line is considered here with heights $[5, 5.3, 5.6]$ m and $[5, 5.3, 6.3]$ m. The resulting PULP for the two configurations differ less than 5%, so that the camber can actually be neglected.

Having settled these issues, before using these tools for assessing the infrastructure impact, it is profitable to apply TLT results in order to check whether the negligible-resonances condition stated in the standard EN 50121 holds. This condition requires that the energy associated with backward-traveling modes must be negligible with respect to the forward-traveling ones. This problem is actually dominated by the less attenuated mode; hence, it suffices to analyze it by defining a sort of reflection coefficient Γ_m whose modulus depends on the line length as

$$\Gamma_m \leq e^{-2\alpha_0 \mathcal{L}} \quad (8)$$

where α_0 is the attenuation constant for the less attenuated mode. This result could be regarded as too conservative. Anyway, applying it to a three-conductor line (i.e., by simplifying an actual railway line by reducing equipotential conductors), the dominant mode is indeed the one describing the differential propagation between the catenary and the rails, which coincides with the least attenuated. Since the propagation mainly follows this pattern, condition (8) is expected to be representative of the actual propagation.

Equation (8) has then been used in order to compute the minimum length required to have negligible reflections, taking $\Gamma_m < 0.3$ (-10 dB) as a reasonable value. The results of this operation are shown in Fig. 5, compared to the 3-km length suggested by the standard: it is interesting to notice that below 1 MHz, the required length is far greater than 3 km, and it can attain very large values in the lower frequency range. In other words, these structures are not as lossy as assumed by the standard; therefore, the potential excitation of resonances is underestimated by the standard. A further condition worsens this scenario: the spectrum of conducted EMI generated by switched-mode devices is usually richer below 1 MHz (depending on the modulation scheme of the switched-mode converter), so that there is a nonnegligible possibility that the indirect contribution from conducted EMI be amplified by resonances.

IV. EXPERIMENTAL VALIDATION

The model introduced here has been validated through experimental tests performed on actual railway lines. The basic configuration of the setup is shown in Fig. 6. The aim is to measure the lateral component of the magnetic field as excited by a function generator connected to the line under test (LUT), between the overhead line (through an isolating hooked stick connected to a metallic wire) and the two rails short-circuited together, while at

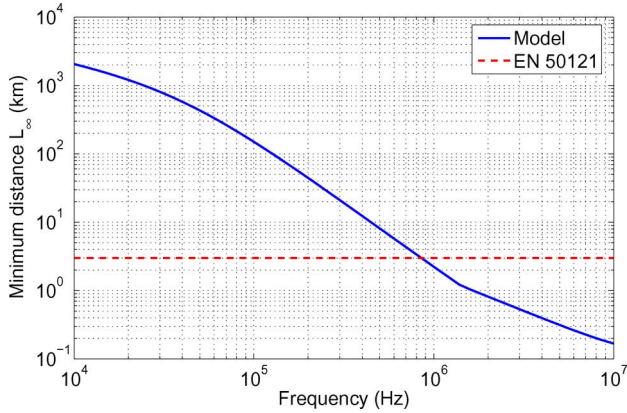


Fig. 5. Simulation results for the minimum length \mathcal{L}_∞ required to regard a railway line as resonance-free.

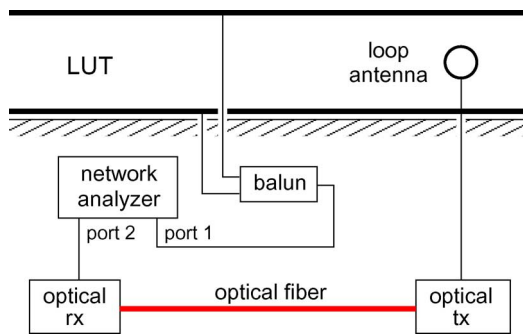
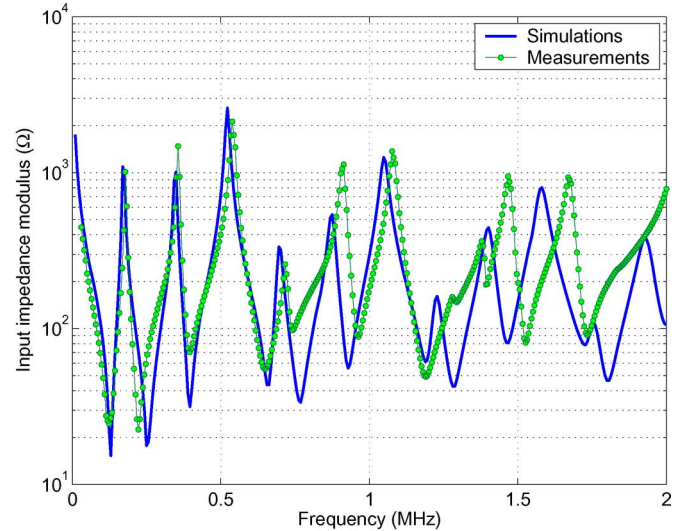


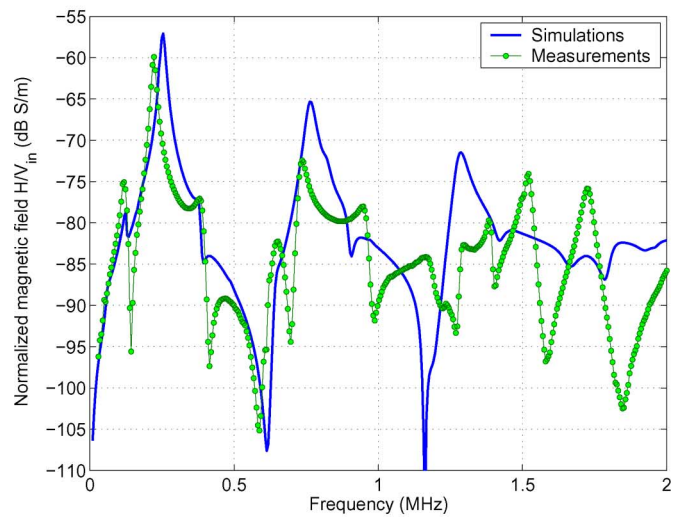
Fig. 6. Measurement setup for the experimental validation on an actual railway line.

the same time, the input impedance of the line, as seen through the output port of the sine-wave generator, is measured, in order to have a trace of the frequency dependence of propagation along the LUT. The use of a network analyzer (NA), although requiring due attention in a high-voltage environment, allows a noise rejection far greater than with asynchronous schemes, e.g., with a spectrum analyzer (SA), while providing a greater sensitivity. One problem with this setup is the need to link the loop antenna and the NA. The simplest solution would be the use of a coaxial cable running along the LUT, but ultimately leading to perturbations in the magnetic field measurements. This problem was avoided by using an optical fiber link. A balun based on a wide-frequency transformer (3-dB passband over 1 kHz–30 MHz) was employed for the excitation of the LUT in order to ensure an ideally differential excitation and a galvanic isolation between the LUT and the NA. The need for a differential excitation is justified by its easier modeling, thus ensuring a more meaningful comparison between experimental and theoretical results.

Several tests were carried out, mainly on two sites: at the CEF and at a facility at Alstom Transport, both in Valenciennes, France. Unfortunately, strong constraints (of commercial and safety nature, time schedule, and so on) make tests on commercial lines, rather than on facilities, very unlikely. Therefore, no experimental validation has been carried out on lines longer than 3 km. Moreover, even the two aforementioned facilities



(a)



(b)

Fig. 7. Experimental results for (a) the input impedance and (b) the magnetic field measured on an Alstom Transport site.

were seldom available, and if available, then for very short sessions; hence, just a small number of tests were performed.

The results presented here refer to the Alstom site, which is 835 m long, with a four-wire catenary and a rock ballast about 30 cm thick; the LUT was electrically disconnected from any power source such as power supply substations. Some results from the validation are shown in Fig. 7; the NA was connected to the line 285 m away from its left end, while the antenna stood at 240 m, 5 m away from the line axis, 1.4 m above the soil. Both the line ends were open-circuited.

The agreement between theory and measurements is satisfactory up to 700 kHz, with errors in the magnetic field computation limited to less than 5 dB. The results on the input impedance Z_{in} actually show that the propagation is also well modeled over the range 1–1.2 MHz; therefore, the current distribution is expected to be properly identified. Nevertheless, the trend in the magnetic field is not correctly predicted in this case: this means

that the disagreement over this frequency range was likely due to limitations in the validity of the radiation formulas. A closer look at the way the disagreement evolves in Z_{in} shows that it is likely due, at least, to an increasing error in the evaluation of propagation constants, as pointed out by the increasing shift in the maxima and minima. This is likely due to our having neglected the dielectric nature of the ballast, as to the fact that the length of the line is just known to a 2% degree of accuracy.

V. ASSESSMENT OF THE INFRASTRUCTURE IMPACT

In order to model radiated emission results, equivalent models are needed for the train too. Actually, the very idea of modeling a train in the frequency domain may look incongruous with the fact that switched-mode regulators have a strong nonlinear behavior. Nevertheless, such an approach is valid in a steady-state analysis, as in this context. In particular, nonlinear circuits performing modulation/regulation can be analyzed by means of Fourier series [5], [22], assessing the spectrum of the conducted emissions they generate, according to the modulation scheme they implement. The resulting spectrum is almost independent of the load characteristics, but for the power factor seen by the switched-mode circuit [5], even above the 1-MHz region. In particular, a switched-mode converter can be represented, for the sake of conducted EMI, as an independent voltage generator in series with an impedance Z_t . While the generator accounts for the conducted EMI spectrum, the impedance Z_t represents all the remaining linear parts of the converter, such as wiring, EMI filters, and so on [23]–[25]. The resulting equivalent circuit is thus valid just as a small-signal model, implying the linearization of the nonlinear systems in a steady-state configuration.

Supposing to have such an equivalent model, we could compute the magnetic field that would be measured by an observer. By performing this operation for the actual site and for the case where the train is connected to an infinite uniform line (the ideal site envisaged by the standard), the infrastructure impact $W(f)$ could be defined as

$$W(f) = \frac{|H_a(f)|}{|H_i(f)|} \quad (9)$$

where $H_a(f)$ and $H_i(f)$ are the magnetic fields for, respectively, the actual and the ideal lines, as measured from the observer position. The function $W(f)$ therefore assesses how the magnetic field spectrum is distorted by the fact of having carried out the tests along a nonideal railway line. Values greater than 1 indicates that the actual site resonances are indeed worsening the indirect radiated EMI of the train, with the risk of regarding it as noncompliant. Unfortunately, to the best of our knowledge, equivalent circuits for conducted EMI are not available for trains. However, thanks to the near-independence of the equivalent circuit from its loading impedance [5], $W(f)$ can be assessed by introducing the site transfer function $\beta(f)$

$$H(f) = \beta(f)I_{in}(f) \quad (10)$$

where I_{in} is the current injected by the train through the pantograph (Fig. 8). The infrastructure impact can now be expressed

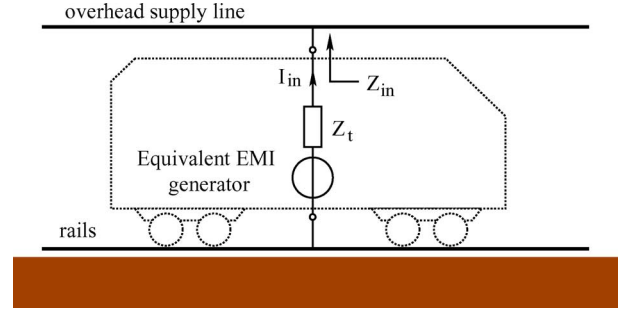


Fig. 8. Equivalent circuit representation used in the assessment of the infrastructure impact $W(f)$.

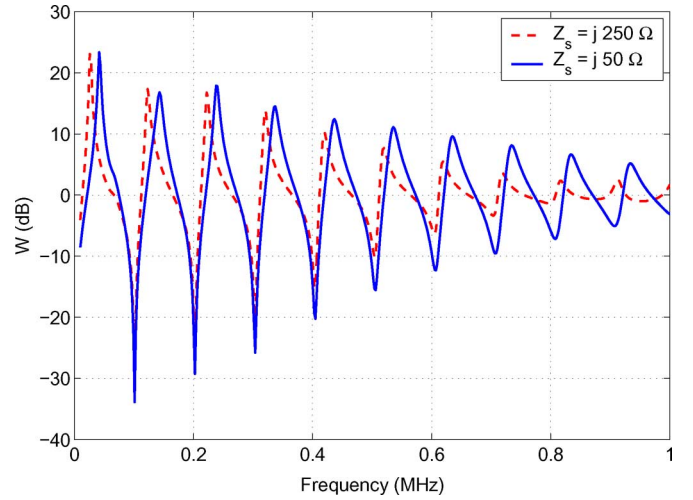


Fig. 9. Distortion factors showing the infrastructure impact for an open-circuited line 3 km long, with the train in the middle of the track. The magnetic field has been computed 10 m away from the line, 2 m high above the soil, and 50 m at the right of the train. Two equivalent internal train impedances have been considered.

as

$$W(f) = \frac{|H_a(f)|}{|H_i(f)|} = \frac{|\beta_a(f)|}{|\beta_i(f)|} \frac{|Z_t(f) + Z_{in,i}(f)|}{|Z_t(f) + Z_{in,a}(f)|} \quad (11)$$

where $Z_{in}(f)$ is the input impedance of the track, as seen from the train between the catenary and the rails. This kind of approach has the advantage of not requiring the knowledge of the equivalent voltage generator, but just of its internal impedance, by invoking the low sensitivity to the site configuration of the equivalent EMI generator. It is important to recall that the train impedance Z_t is independent of the input impedance of the line $Z_{in}(f)$, since it is just related to linear circuits.

An example of results obtained with this procedure is shown in Fig. 9, where the actual site is a uniform track 3 km long, with open-circuited ends, and the train placed in the middle of the track. The internal impedance Z_t of the train has been assumed to be inductive, considering the two values $50j \Omega$ and $250j \Omega$. These values are not meant to be representative of an actual train; they are just considered as an example for discussing the infrastructure impact $W(f)$. As a matter of fact, Z_t can be expected to be strongly dependent on frequency, much in the

same way as for the high-frequency behavior of a low-frequency transformer.

The results in Fig. 9 are quite self-explaining; indeed, resonances can distort the results of the radiated emissions test, in two respects: the most evident effect is the increase in the maxima, which can easily exceed 10 dB. But this is not the only effect, since whenever important conducted EMI harmonics occur at the same frequency as a minimum in the transfer function, their importance can be underestimated. This eventuality, although unlikely, represents a treat to the effectiveness of the standard, since noncompliant trains could not be identified as such, if tested on certain railway sites.

VI. EXPERIMENTAL CHARACTERIZATION OF A RAILWAY LINE

Unfortunately, three obstacles impede the use of a predictive model: 1) the literature is very poor about high-frequency equivalent models for power devices, which may be required to be characterized under a high-voltage supply; 2) not even the site owner is able to provide an accurate description of the test site, not only from a geometrical point of view, but also regarding the presence of partially hidden power devices such as for over-voltage protection; 3) because of the very feeble propagation attenuation in the lower frequency range, portions of the site physically very distant (several 10 km) from the TUT may have a nonnegligible effect on the overall infrastructure impact; since this would require a very large extension of the site to be modeled, the work required to describe it would be hardly justified. These three points are a formidable challenge to any actual modeling attempt. Therefore, predictive models are more likely to be useful as reference tools to understand the phenomena involved in the excitation of radiated emissions, or during design sessions.

On the other hand, a more feasible approach is proposed here. Rather than pursuing a predictive simulation, an equivalent model of the site can be derived from experimental measurements with *no a priori* information. The first step to be undertaken is to identify a portion of line clear of any significant discontinuities that will be referred to as the reference line. Since the tests are to be carried out in a steady-state configuration, all the power devices connected to the remaining portion of the test site can be described through Thévenin-like equivalent circuits. Hence, because the rest of the elements in a test site are linear, a more general equivalent circuit can be defined representing the entire test site outside the reference line where the TUT lies by means of two equivalent circuits (Fig. 10). Once these two circuits are available, the entire actual system can be accurately simulated; on the other hand, the response of the ideal site can be easily estimated by substituting these two equivalents with the characteristic impedance matrix of the reference line, thus simulating an infinite line.

In order to estimate the two equivalents, we here propose a procedure based on magnetic field measurements by defining the inverse problem

$$\mathbf{H}_m = \mathbf{f}(\mathbf{p}) \quad (12)$$

where \mathbf{p} is a vector containing the unknown parameters defining the equivalent circuits, \mathbf{H}_m is a vector of magnetic

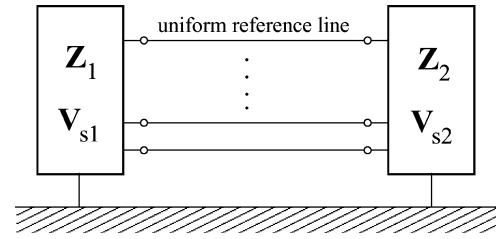


Fig. 10. Equivalent site representation sought here, based on the identification of a reference uniform line.

field measurements (amplitude-only data from the SA), and $\mathbf{f}(\cdot)$ is a function relating the equivalent description of the site (through the uniform line and the set of parameters \mathbf{p}) to the theoretical magnetic field. This last operation employs the previously introduced model in a predictive way. The equals sign in (12) is to be taken in a weak sense, as we have chosen to look for a least square solution.

The proposed approach consists of two steps: 1) collecting the data and 2) solving an optimization problem through predictive simulations. The first point is accomplished by exploiting the ambient noise of the site; as a matter of fact, this background magnetic field, mostly excited by conducted EMI propagating along the supply line and generated by substations and other trains, contains information about the electrical configuration of the entire site. The second step deals with an optimization problem aiming at solving (12) through the minimization of the error function $e(\mathbf{p})$

$$e(\mathbf{p}) = \|\mathbf{H}_m - \mathbf{f}(\mathbf{p})\|_2. \quad (13)$$

The feasibility of this latter task strongly depends on the amount and quality of available experimental data. Conversely, as for many inverse problems, the solution of this problem is unstable, due to its ill-posed nature: indeed, there exists a number of electrical configurations that can provide very similar results. During the “inversion,” this leads to a strong sensitivity of the equivalent parameters with respect to the magnetic field measurements. Two actions are to be taken in order to reduce this instability: by increasing the amount of uncorrelated magnetic field measurements, we get more information on the electrical configuration we are looking for, whereas by introducing *a priori* information, the problem is regularized, i.e., its sensitivity is reduced.

In order to actually collect meaningful information, the magnetic field samples should be measured at least at a distance of $\lambda/10$ from each other; satisfying this requirement implies that the length of the reference line should be proportional to the maximum wavelength, corresponding to the minimum frequency of interest. Considering a few tens kilohertz, this would mean to consider several tens kilometers, which would require the antenna and the SA (together with their energy supply) to be moved along this distance. Practical aspects would limit the reference line to a few hundred meters: therefore, samples in the lower frequency range will be quite similar, thus with a limited amount of information. More information can be obtained by locally modifying the electrical configuration of the test site. By adding lumped loads at the ends of the reference line, the

measured magnetic field will be modified too; nevertheless, it will still depend on the rest of the site, i.e., the configuration we are interested in, while bringing additional data. Practically, this idea would require the use of a high-voltage decoupling capacitor inserted between the load and the overhead line (by means of an isolating hooked stick), thus allowing the use of low-voltage loads. High-capacitance power isolators could be used as decoupling capacitors. The aim here is to introduce a perturbation that will just be seen from the EMI viewpoint, while the power electronics will still see the same low-frequency loads, so as to ensure the time invariance of the system.

On the other hand, the inverse problem can be regularized by reducing the degrees of freedom. For instance, passivity should be enforced by requiring the impedance matrices \mathbf{Z} to have a positively definite real part. Furthermore, symmetry can be exploited, e.g., one can rightfully assume the two rails to be electrically symmetrical. Finally, the number of unknowns can be decreased by reducing the overhead line to a single conductor. The simplest solution to the inverse problem follows a trial-and-error scheme. At each run, the vector \mathbf{p} is randomly generated as a guess value: these parameters identify a certain electrical configuration of the site. By applying the previous model in a predictive way, the magnetic field is estimated at the same locations where it has been actually measured. This first phase is usually referred to as direct solution. This operation is carried out for a certain number of runs, then a minimum search method is applied, keeping track of the partial solution giving the lowest value for the error $e(\mathbf{p})$. The random approach allows a rough inspection of the solution space defined by \mathbf{p} , which is characterized by widely variable parameters, e.g., impedance can range from a short circuit to an open one, due to the resonant nature of the system. This approach is far from optimal, and its poor performance are worsened by the fact that there is no assurance to find the global minimum. Actually, the aim here was just to prove the feasibility of this approach, while actual implementations for industrial applications will require further investigations in order to effectively solve the inverse problem with an acceptable confidence margin. Furthermore, we had no possibility to carry out experimental validations, which justifies the all-numerical investigation.

A numerical feasibility test for this approach has been carried out by considering the railway line in Fig. 11(a). Five magnetic field samples have been computed along the 700-m reference line. In order to increase the amount of data, nine load configurations have been applied to the ends of the reference line, considering three loads: an open circuit, and a 50- and a 300- Ω resistance, making a grand total of 45 spectra. The two equivalent circuits have been estimated just up to 200 kHz, since at higher frequencies, the inverse problem is expected to be less critical. From this equivalent representation, the magnetic field has been computed for the two configurations shown in Fig. 11(b), where the TUT is represented as a Thévenin-like equivalent. The results of this operation are shown in Fig. 12, as obtained from 50 runs, compared with the results obtained by simulating the original description in Fig. 11(a). Indeed, the trend in the spectra is fairly well identified, even though there are important disagreements: in particular, as expected, in the lower frequency

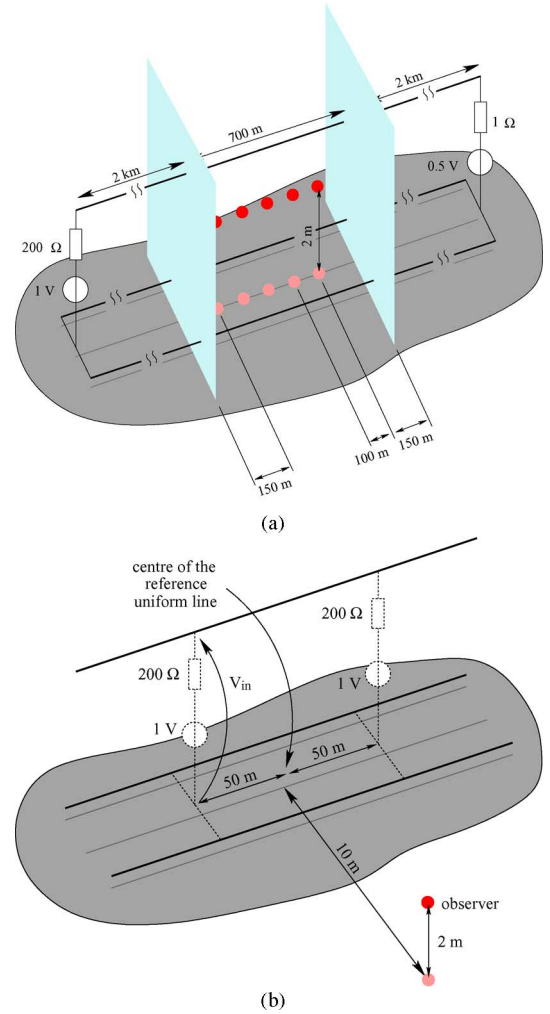


Fig. 11. Feasibility test for the experimental site characterization. (a) Three-wire line considered for the numerical validation of the site characterization approach. The reference uniform line as defined by two reference planes, together with the five positions where the magnetic field is measured. (b) Two configurations tested for validating the site characterization.

range. Beside the validation of the characterization procedure, the infrastructure impact has been pointed out by substituting the two equivalent representations at the uniform line ends with the characteristic impedance matrix \mathbf{Z}_c ; the magnetic field computed for this configuration is also shown in Fig. 12. Therefore, a procedure as the one described here would allow the manufacturer to characterize a site before actually testing the train, providing a tool for assessing the impact of the infrastructure.

Nevertheless, in order to make an industrial tool out of this idea, one should find a way to ensure, up to a certain degree, the convergence of the optimization routine toward the global minimum. A likely way to improve it is to apply a simulating annealing approach, which generalizes the idea of a random search for the global minimum, but gradually reducing its range of variability, thus providing a sort of convergence, even without ensuring the ability to find the global minimum. Besides, a better optimization routine would also relax the need for information, and in particular, it could lead to a measurement routine without the need to apply load pairs; this would make

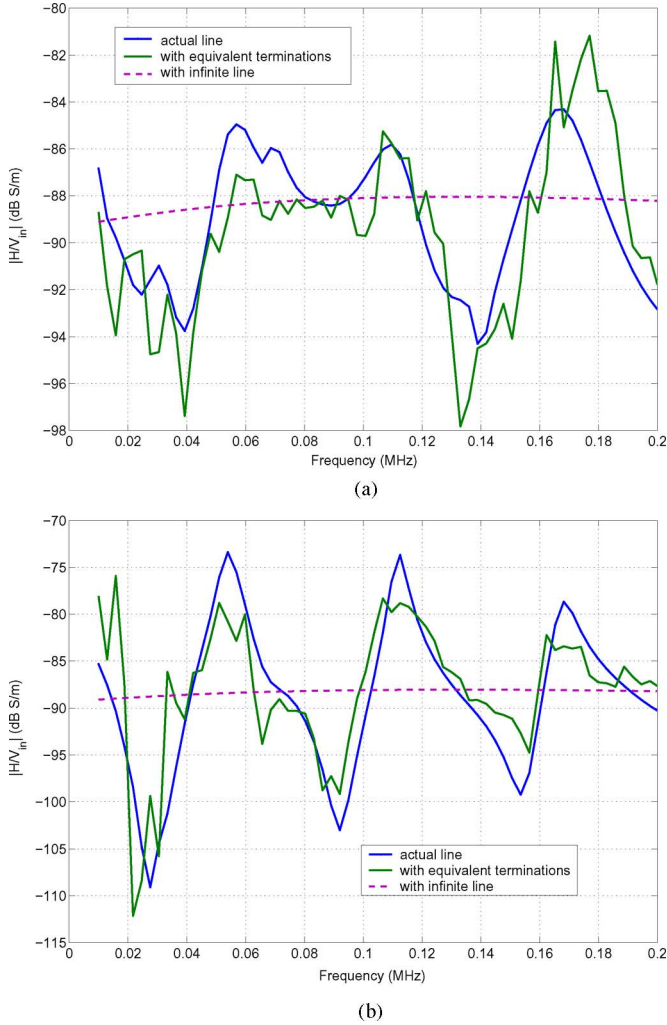


Fig. 12. Results of the numerical validation for the experimental site characterization, showing the magnetic field computed for the system in Fig. 11(a) and the one computed by using its equivalent characterization. Two positions are considered for the train. (a) Left side of the uniform line. (b) Right side. The magnetic field that would have been obtained with an infinite line is also shown.

an even stronger case for the use of this characterization technique. This approach indirectly implies the time invariance of the site, whose equivalent electrical configuration is not supposed to vary significantly between the site characterization and the testing of the train. Such hypothesis could prove not to hold when considering sites with trains moving or changing the loading of power supply substations.

VII. CONCLUSION

In this paper, we have addressed the problem of modeling electric railway lines in order to assess the infrastructure impact in testing radiated emissions of rolling stock. In the first part, we proposed the use of a theoretical description of the test site where the train is to be tested. By simulating the response of the actual site and comparing it with the ideal resonance-free site envisaged by the standard EN 50121, one can distinguish between excessive magnetic field values due to the train or rather due to resonances of the infrastructure. The model described

here has shown to be accurate enough when applied to actual railway lines up to 700 kHz, even with the introduction of approximations for the treatment of nonidealities of railway lines (overhead line reduction, ballast, cambers, etc.).

This model has then been used to check the accuracy of the negligible-resonance hypothesis stated in the standard, proving its inaccuracy and the subsequent underestimation of infrastructure resonances, due to the overestimation of propagation attenuation. This, together with the difficulties in getting a fair description of the test site and of related power devices, has pointed out the strong limitations any modeling efforts are bound to encounter. For these reasons, we have finally proposed an alternative experimental characterization based on magnetic field measurements with no *a priori* information of the actual site configuration. The feasibility of this approach has been demonstrated through a numerical study, emphasizing the limitations due to the numerical solution of this inverse problem. Although further investigations have to be carried out, an improved version of this approach currently seems to be the only practical way of characterizing a railway site, and subsequently of assessing the impact of its configuration in radiated emissions tests.

APPENDIX

A. PULP for an MTL Above a Lossy Soil

The following expressions refer to results presented in [13]. For the sake of simplicity, the notation is simplified here, though referring to the quasi-static solution obtained under a logarithmic approximation [17]

$$\mathbf{A} = (\mathbf{\Lambda} + 2\mathbf{S}_2^h)^{-1} (\mathbf{\Lambda} + 2\mathbf{S}_1^h) \quad (14)$$

$$\mathbf{Z}_e = \frac{j\omega\mu_0}{2\pi} \mathbf{\Lambda} \quad (15)$$

$$\mathbf{Y}_e = j\omega\epsilon_0 2\pi \mathbf{\Lambda}^{-1} \quad (16)$$

$$\mathbf{Z}_g = \frac{j\omega\mu_0}{\pi} (\mathbf{S}_1^h - \mathbf{S}_2^0 \mathbf{A}) \quad (17)$$

$$\mathbf{Y}_g = j\omega\epsilon_0 \pi (\mathbf{S}_2^h - \mathbf{S}_2^0)^{-1} \quad (18)$$

The quasi-static approximation of the remaining matrices is given by

$$\Lambda_{ik} \simeq \frac{1}{2} \ln \left[\frac{h_+^2 + d^2}{h_-^2 + d^2} \right] \quad (19)$$

$$S_{1,ik}^h \simeq \frac{1}{4} \ln \left[\frac{(h_+ + c_1)^2 + d^2}{h_+^2 + d^2} \right] \quad (20)$$

$$S_{2,ik}^h \simeq \frac{1}{2(1 + \tilde{\epsilon})} \ln \left[\frac{(h_+ + c_2)^2 + d^2}{h_+^2 + d^2} \right] \quad (21)$$

$$S_{1,ik}^0 \simeq \frac{1}{4} \ln \left[\frac{(h_i + c_1)^2 + d^2}{h_i^2 + d^2} \right] \quad (22)$$

$$S_{2,ik}^0 \simeq \frac{1}{2(1 + \tilde{\epsilon})} \ln \left[\frac{(h_i + c_2)^2 + d^2}{h_i^2 + d^2} \right] \quad (23)$$

where $h_{\pm} = h_k \pm h_i$, $d = d_k + r_k - d_i$, and with $\beta = \gamma_0(\tilde{\epsilon} - 1)$, $c_1 = 2/\beta$, $c_2 = (1 + \tilde{\epsilon})/\beta$, $\gamma_0 = jk_0$ being the free-space propagation constant.

B. Magnetic Field Near an MTL Above a Lossy Soil

These results have been originally presented in [16]

$$\Theta_{ik} = \frac{1}{\pi} (-\Upsilon_{ik} + k_0^2 \mathcal{J}_{1,ik} + \gamma_k^2 \mathcal{J}_{2,ik} + \mathcal{J}_{3,ik}) \quad (24)$$

with

$$\Upsilon_{ik} = \frac{\Gamma_k}{2} \left[\frac{x_o + h_i}{\rho_{+,i}} K_1(\Gamma_k \rho_{+,i}) - \frac{x_o - h_i}{\rho_{-,i}} K_1(\Gamma_k \rho_{-,i}) \right] \quad (25a)$$

$$\mathcal{J}_{1,ik} = \int_0^\infty \frac{\phi_1}{u_{0,k}} \cos[\lambda(y_o - d_i)] d\lambda \quad (25b)$$

$$\mathcal{J}_{2,ik} = \int_0^\infty \frac{\phi_\varepsilon}{u_{0,k}} \phi_\varepsilon \cos[\lambda(y_o - d_i)] d\lambda \quad (25c)$$

$$\mathcal{J}_{3,ik} = \int_0^\infty \lambda^2 \frac{\phi_1}{u_{0,k}} \cos[\lambda(y_o - d_i)] d\lambda \quad (25d)$$

where $K_1(\cdot)$ is the modified Bessel function of the second type, first-order, $\Gamma_k^2 = \gamma_0^2 - \gamma_k^2$, and the kernels ϕ are to be read as $\phi(\gamma_k, x_o + h_i, \lambda)$, having defined

$$\phi_\chi(\gamma_k, x, \lambda) = \frac{e^{-u_{0,k} x}}{\chi u_{0,k} + u_{g,k}} \quad (26)$$

with $u_{0,k}^2 = \lambda^2 - \gamma_k^2 + \gamma_0^2$, $u_{g,k}^2 = \lambda^2 - \gamma_k^2 + \tilde{\varepsilon} \gamma_0^2$, and $\rho_{\pm,i}^2 = (x_o \pm h_i)^2 + (y_o - d_i)^2$.

ACKNOWLEDGMENT

This work was carried out during the Ph.D. thesis of the first author under an agreement between Alstom Transport (St. Ouen, France), CEF (Valenciennes, France), the Politecnico di Torino (Turin, Italy), and IEMN/TELICE.

REFERENCES

- [1] T. Konefal, D. A. J. Pearce, C. A. Marshman, and L. M. McCormack *Potential Electromagnetic Interference to Radio Services From Railways*, Radiocommun. Agency, 1st issue, York EMC Services Ltd., Univ. York, York, U.K., Final Rep. AY4110.
- [2] *Railway Applications—Electromagnetic Compatibility*, CENELEC Standard EN 50121, 2006.
- [3] R. J. Hill, "Electric railway traction: Part 3. Traction power supplies," *Inst. Electr. Eng. Power Eng. J.*, vol. 8, no. 6, pp. 275–286, Dec. 1994.
- [4] P. Chapas, *Traction Ferroviaire*. Levallois-Perret Cedex, France: Alstom Transport, Sep. 1999.
- [5] L. Tihanyi, *Electromagnetic Compatibility in Power Electronics*. Piscataway, NJ: IEEE Press, 1995.
- [6] A. Cozza, "Railways EMC: Assessment of infrastructure impact," Ph.D. dissertation, Université des Sciences et Technologies de Lille, Lille, France, Jun. 22, 2005. (Available at request from the authors)
- [7] E. F. Vance, *Coupling to Shielded Cables*. New York: Wiley, 1977.
- [8] H. Kuester, D. C. Chang, and R. G. Olsen, "Modal theory of long horizontal wire structures above the Earth. 1. Excitation," *Radio Sci.*, vol. 13, no. 4, pp. 556–557, Jul./Aug. 1978.
- [9] R. M. Sorbello, R. W. P. King, K. M. Lee, L. C. Shen, and T. T. Wu, "The horizontal-wire antenna over a dissipative half-space: Generalized formula and measurements," *IEEE Trans. Antennas Propag.*, vol. AP-25, no. 6, pp. 850–854, Nov. 1977.
- [10] P. Degauque, G. Courbet, and M. Heddebaut, "Propagation along a line parallel to the ground surface: Comparison between the exact solution and the quasi-TEM approximation," *IEEE Trans. Electromagn. Compat.*, vol. EMC-25, no. 4, pp. 422–427, Nov. 1983.
- [11] C. R. Paul, *Analysis of Multiconductor Transmission Lines*. New York: Wiley, 1994.
- [12] J. R. Carson, "Wave propagation in overhead wires with ground return," *Bell Syst. Tech. J.*, vol. 5, pp. 539–554, 1926.
- [13] M. D'Amore and M. S. Sarto, "Simulation models of a dissipative transmission line above a lossy ground for a wide frequency range—Part II: Multiconductor configuration," *IEEE Trans. Electromagn. Compat.*, vol. 38, no. 2, pp. 139–149, May 1996.
- [14] J. R. Wait, "Theory of wave propagation along a thin-wire parallel to an interface," *Radio Sci.*, vol. 7, no. 6, pp. 675–679, Jun. 1972.
- [15] G. E. Bridges and L. Shafai, "Validity of the thin-wire approximation of conductors near a material half-space," in *Antennas Propag. Soc. Int. Symp., AP-S Dig.*, Jun. 26–30, 1989, pp. 232–235.
- [16] M. D'Amore, M. S. Sarto, and A. Scarlatti, "Theoretical analysis of radiated emission from modal currents in multiconductor transmission lines above a lossy ground," in *Proc. IEEE Int. Symp. Electromagn. Compat.*, Aug. 21–25, 2000, vol. 2, pp. 729–734.
- [17] P. Pettersson, "Image representation of propagation of transients on overhead transmission lines," presented at the Cigré Symp., Lausanne, Switzerland, Oct. 1993, Paper 200-08.
- [18] S. L. Marple, *Digital Spectral Analysis: With Applications*. Englewood Cliffs, NJ: Prentice-Hall, 1986.
- [19] J. R. Wait, *Electromagnetic Wave Theory*. New York: Harper & Row, 1985.
- [20] R. J. Hill and D. C. Carpenter, "Rail track distributed transmission line impedance and admittance: Theoretical modeling and experimental results," *IEEE Trans. Veh. Technol.*, vol. 42, no. 2, pp. 225–241, May 1993.
- [21] A. Mariscotti and P. Pozzobon, "Synthesis of line impedance expressions for railway traction systems," *IEEE Trans. Veh. Technol.*, vol. 52, no. 2, pp. 420–430, Mar. 2003.
- [22] J. A. Taufiq and J. Xiaoping, "Fast accurate computation of the DC-side harmonics in a traction VSI drive," *Proc. Inst. Electr. Eng.*, vol. 136, no. 4, pp. 176–187, Jul. 1989.
- [23] R. J. Hill, "Electric railway traction: Part 6. Electromagnetic compatibility—Disturbance sources and equipment susceptibility," *Inst. Electr. Eng. Power Eng. J.*, vol. 11, no. 1, pp. 31–39, Feb. 1997.
- [24] J. Shen, J. A. Taufiq, and A. D. Mansell, "Analytical solution to harmonic characteristics of traction PWM converters," *Inst. Electr. Eng. Proc. Electr. Power Appl.*, vol. 144, no. 2, pp. 158–168, Mar. 1997.
- [25] X. Pei, K. Zhang, Y. Kang, and J. Chen, "Analytical estimation of common mode conducted EMI in PWM inverter," in *Proc. 26th Annu. Int. Telecommun. Energy Conf. (INTELEC 2004)*, Sep. 19–23, pp. 569–574.



Andrea Cozza (S'02–M'05) received the Laurea degree (*summa cum laude*) in electronic engineering from the Politecnico di Torino, Turin, Italy, in 2001, and the Ph.D. degree in electronic engineering from the Politecnico di Torino and the University of Lille, Lille, France, in 2005.

In 2007, he joined the Electromagnetics Research Department, L'École Supérieure d'Électricité (SUP-ELEC), Gif sur Yvette, France, as a Researcher and an Assistant Professor. His current research interests include modeling of transmission lines, near-field measurement techniques, reverberation chambers, electromagnetic dosimetry, and applications of time-reversal to electromagnetics.



Bernard Démoulin was born in Denain, France, on November 7, 1946. He received the M.S. and Ph.D. degrees from the Université de Sciences et Technologies de Lille, Villeneuve d'Ascq Cedex, France, in 1971 and 1973, respectively.

He is currently a Professor at the Université de Sciences et Technologies de Lille, where he works with the Telecommunication, Interferences and Electromagnetic Compatibility (TELICE) Group, Institut d'Électronique, de Microélectronique et de Nanotechnologie (IEMN) Laboratory. His current research interests include electromagnetic compatibility measurements especially in mode-stirred reverberation chambers and electromagnetic coupling computation throughout multiple-wire cables, as well as the characterization of integrated circuits in terms of susceptibility.

Prof. Démoulin is a Senior Member of the French Electrical Engineering Society (SEE) and a correspondent of the International Scientific Radio Union (URSI).

On the Modeling of Electric Railway Lines for the Assessment of Infrastructure Impact in Radiated Emission Tests of Rolling Stock

Andrea Cozza, *Member, IEEE*, and Bernard Démoulin

Abstract—In this paper, we address the problem of testing radiated emissions generated by rolling stock, when carried out on actual railway sites, as prescribed by the standard EN 50121. The idea of assessing infrastructure impact on test results is presented here by means of an electromagnetic model of railway sites. In the first part, modeling tools are introduced together with some results from the experimental validation. These tools are then applied to actual railway lines proving the importance of site resonances and the ambiguities in the application of the standard EN 50121 in the industrial domain. After pointing out the main difficulties in the simulation of actual railway sites, we present a feasibility study of an alternative procedure for the modeling of a site, based on magnetic field measurements and the solution of an inverse problem with no *a priori* information about the test site configuration.

Index Terms—Electromagnetic (EM) radiation, inverse problems, multiconductor transmission lines, standards, transportation.

I. PROBLEM DESCRIPTION AND INDUSTRIAL BACKGROUND

THE DRAMATIC increase in the use of electronic devices in almost any domain has led to a substantial rise of the potential for interference between equipment working in the same environment. Because of the likely disruptions that may follow this scenario, electromagnetic compatibility (EMC) has established itself as the cornerstone for the proper working of any electronic equipment.

The railway domain has been part of this trend since the early introduction of static conversion through power transistors acting as switches, through switched-mode conversion/regulation, that generates strong current/voltage gradients leading to interference phenomena that could jeopardize the proper working of electronic devices within the train itself and the correct interpretation of railway control signals propagating along the rails. This is a major issue because of the inherent security hazards involved: the failing of security and control devices could have dire consequences. This was a major point for the introduction of EMC testing of rolling stock. Moreover, electromagnetic in-

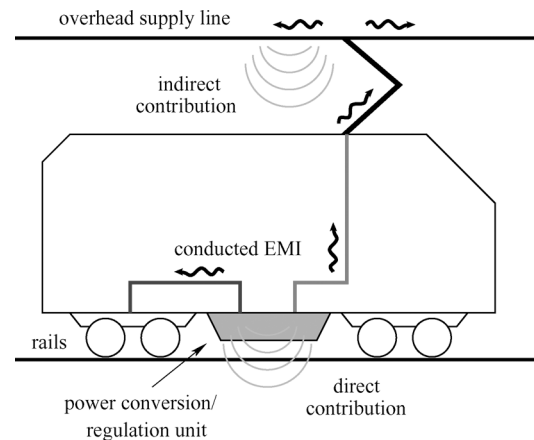


Fig. 1. Schematic representation showing the main interference phenomena generated by the switched-mode conversion unit onboard an electric train.

terference (EMI) can affect, through radiation and propagation, other systems not directly related to the railway domain, such as telecommunications lines and wireless systems [1]. Typical maximum levels of the magnetic field imposed by the standard are of the order of $45 \text{ dB} \cdot \mu\text{A}/\text{m}$ at 100 kHz, as measured by a 200-Hz bandwidth receiver [2]. The actual masks imposed depend on the frequency as well as on the railway infrastructure and technology.

The main phenomena involved in the EMC of electric trains can be broadly summarized through the paradigm introduced in Fig. 1, depicting a train supplied by an overhead line. The absorbed electrical energy is converted and/or regulated by a switched-mode unit, in order to ensure all the different electrical energy supplies required for its functioning. The inherently strong current and voltage time derivatives generate conducted EMI that propagate along the internal cabling: part of them will affect other devices inside the train itself, whereas another part will reach the train pantograph and then the supply line, thus affecting the world outside the train. On the other hand, the switched-mode unit will also directly excite an electromagnetic (EM) field outside the train, thus giving place to radiated EMI. Nevertheless, these are not the only effects caused by EMI generated by the train: as a matter of fact, the current injected into the supply line (overhead wires, rails, ground wires), and propagating along it, is bound to give an indirect contribution to the overall EM field excited by the train. Therefore, it is no wonder that EMC standards have been introduced, dealing with the generation of EMI. Their main aim is to set maximum levels

Manuscript received June 18, 2007; revised December 21, 2007.

A. Cozza is with the Electromagnetics Research Department, L'École Supérieure d'Électricité (SUPELEC), 91192 Gif-sur-Yvette, France (e-mail: andrea.cozza@supelec.fr).

B. Démoulin is with the Telecommunication, Interferences and Electromagnetic Compatibility (TELICE), Institut d'Électronique, de Microélectronique et de Nanotechnologie (IEMN) Laboratory, Université de Sciences et Technologies de Lille, 59655 Villeneuve d'Ascq Cedex, France (e-mail: bernard.demoulin@univ-lille1.fr).

Color versions of one or more of the figures in this paper are available online at <http://ieeexplore.ieee.org>.

Digital Object Identifier 10.1109/TEMC.2008.924387

for conducted and radiated EMI generated by rolling stock and power supply substations. In the context of the European Union, the reference in railway EMC is set by the European Committee for Electrotechnical Standardization (CENELEC) standard EN 50121 [2].

The introduction of this standard in 1996 in its experimental version, later updated in 2000, has proven to be a formidable drive toward a stronger commitment to EMC on the manufacturer side. Since trains cannot be tested in standard facilities such as anechoic chambers due to practical problems (dimensions, power supply, etc.), the only practical way of performing these tests is to consider actual railway lines, where the train can be operated more easily.

Actual configurations of railway lines vary, both geometrically, and topologically and electrically [3], [4]: while these differences are not expected to affect the generation of EMI from the train itself [5], which can be indeed regarded as an independent EMI source, they are expected to have by far a greater impact on the indirect contribution to radiated EMI. Therefore, the overall EM field measured near a train would depend in part on the test site configuration. This problem is worsened by the likely excitation of resonances along the supply line, due to low propagation attenuation (see Section III). The excitation of undamped resonances would ultimately lead to sharp maxima in radiated EMI. While dealing with a standard, tests should yield comparable results whatever railway structure they are carried out on. The solution envisaged by the CENELEC committee was to perform the tests related to the train on a line ideally infinitely long, clear of any electrical discontinuities along it, since such a configuration would be the simplest and least ambiguous one to be considered. This is due to the fact that along an infinite uniform line, no reflection can occur, hence no resonances. Although actual sites never fulfill such requirements, they can acceptably approximate them as long as reflections coming back toward the train are negligible, a condition that is met whenever the propagation attenuation is strong enough, i.e., for a lossy line long enough to have reflections reduced to negligible levels. To this end, the CENELEC committee prepared a set of guidelines to be followed in order to minimize the infrastructure impact [2], following the basic idea of obtaining results reproducible on other test sites. In particular, the concept of a minimum length of the test track was introduced.

Considering this scenario, it appears quite obvious why, amid other tests, characterizing radiated emissions near a train is considered a critical task. Whenever the line resonates at a given frequency where the train generates important conducted EMI, relatively strong EM field maxima occur; unfortunately, it is very difficult to decide whether a maximum has been actually “amplified” by the infrastructure or not. This also explains why the customer always requires the manufacturer to perform the tests on his own site, i.e., in order to be sure that the train is standard-compliant on the site where the train will be used, rather than on a generic facility. The standard acknowledges this problem, suggesting an ambient noise characterization by measuring the EM field radiated by the supply line while the train is not yet present. The underlying idea is to exploit the conducted EMI generated by power supply substations as a mean to high-

light the presence of resonances. Eventually, the comparison of the ambient noise spectrum with the actual test results would justify strong peaks in the spectrum measured near the train as due to line resonances. Nevertheless, this would not yield any quantitative information on the infrastructure impact.

This problem is a major issue for the manufacturer, since it can prove to be a tough job to demonstrate to the customer that the excessive radiation of a train is partly due to the test site. Moreover, the guidelines given by the standard cannot always be satisfied, thus increasing the odds of exceeding the standard-imposed limits. Such an outcome can have important repercussions on the manufacturer: delays in the delivery schedule, extra costs in order to reduce seemingly excessive EMI, and so on. These considerations have led Alstom Transport, a rolling stock manufacturer, and the Centre d'Essai Ferroviaire (CEF), a railway test facility, to propose a research project addressing these issues [6]. The aim was to study the phenomena involved in the generation of the EM field near a train, in order to develop a theoretical model for the assessment of the infrastructure impact on test results, by simulating radiated EMI tests along actual test sites and an ideal infinite one, i.e., closed on matched loads. Such a tool could be used as a qualitative and quantitative way of proving to a customer that excessive levels in the measured EM field spectra may be due to the site infrastructure rather than due to the train. This would allow the manufacturer to argue on the consistency of the test methods and results, showing that not all the blame can be put on to him. To this end, this tool should be as simple as possible, while giving sound results. As a matter of fact, it would not be practical to use full-wave simulators due to the sheer dimensions of a railway site; this would require hours of computations, whereas the customer usually allows the manufacturer inside his site only for a very limited amount of time. Furthermore, not even the customer has a detailed description of the actual configuration of his site, so that the model to be used is bound to be an extremely simplified one: this problem is addressed in Section III.

This paper is organized as follows. In Section II, we present the theoretical tools that have been employed for the modeling of uniform railway lines; the difficulties in modeling actual lines are then addressed in Section III, whereas experimental results validating the model are presented in Section IV. Finally, we show how these tools can be utilized for the assessment of the infrastructure impact: first in a predictive way, given a sufficiently detailed equivalent description of the railway site, and then, in an alternative way, based on an experimental characterization of the site, with no *a priori* information.

II. MODELING TOOLS FOR A RAILWAY LINE

Industrial experience within Alstom Transport has shown that resonances pose problems mainly below 1 MHz. The standard EN 50121 only requires the measurement of the y -component H_y (Fig. 2) of the magnetic field up to 30 MHz at a distance of 10 m away from the track axis, with the mechanical center of the loop antenna 1–2 m high above the soil, facing the train under test (TUT). Therefore, our investigations were limited just to H_y up to about 1–2 MHz, by means of near-field antenna

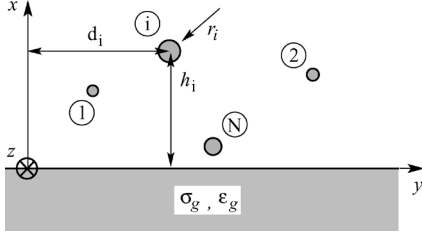


Fig. 2. Railway line as a transmission line structure: cross section.

theory models. Actually, the TUT is to be tested under two basic configurations: a static (no traction devices activated) and a slow motion one. A static configuration will be assumed hereafter; nevertheless, the results obtained in this way can still be used for the slow-motion configuration.

An effective and simple tool for the modeling of line structures is transmission line theory (TLT), based on a quasi-TEM approximation. A good adherence to experimental results is expected as long as each conductor is electrically near to the ground–plane interface. This assumption holds for the typical values h_i encountered in railway lines, over the frequency ranges that we are interested in here. Attention should be given to the fact that soil cannot be approximated as a perfect conductor: in this paper, it will be assumed to be a homogeneous half-space characterized by a complex relative dielectric constant $\tilde{\epsilon} = \epsilon_g - j\sigma_g/(\omega\epsilon_0)$, with $\epsilon_g \in [5, 15]$ and $\sigma_g \in [1, 100]$ mS/m [7]. A typical value is $\sigma_g = 10$ mS/m. A sensitivity analysis [6] has pointed out that ϵ_g has a negligible effect on the overall system behavior, since the soil transition from lossy conductor to lossy dielectric, i.e., $\sigma_g = \omega\epsilon_0\epsilon_g$, occurs above 2 MHz, even for a low-conductivity soil (sandy soils, 1 mS/m). The consequences of a finitely conducting ground–plane have been investigated in many works over the past century; concerning TLT, the validity of the quasi-TEM approximation has been investigated in [8] and [9] from a theoretical point of view and experimentally in [10], showing that the quasi-TEM mode still dominates for conductors electrically close to the soil interface.

Propagation is simply described once per-unit-length parameters (PULP) are known. Simple closed-form expressions are available for an MTL above a lossless ground–plane [11]; nevertheless, the finite soil conductivity modifies these parameters. It was first shown in [12] that the computation of PULP for a lossy soil can be addressed by decomposing it into two parts: the first one corresponds to the external PULP \mathbf{Z}_e , \mathbf{Y}_e , computed by regarding the soil as a perfect conductor, whereas the second part \mathbf{Z}_g , \mathbf{Y}_g accounts for the soil finite conductivity, as

$$\mathbf{Z} = \mathbf{Z}_e + \mathbf{Z}_g \quad (1a)$$

$$\mathbf{Y}^{-1} = \mathbf{Y}_e^{-1} + \mathbf{Y}_g^{-1}. \quad (1b)$$

The closed-form expressions reported in Appendix A have been used, as derived in [13] from the theoretical model proposed in [14]. Those results have been obtained under a thin-wire approximation, which is usually invoked whenever $h/r \gg 1$; although this condition is not satisfied by rails, it has been proven [15] that the actual condition to satisfy is $h_i/r_i > 1$, i.e., for conductors almost in contact with the soil interface. This

condition is actually met by rails too; moreover, the analysis of a railway line can be further simplified by considering equivalent circular rails rather than their actual profile. This would allow the use of all the formulas in Appendix A without any need to employ numerical methods for the computation of the PULP. The estimation of the equivalent rail radius has been carried out in [6]: actual rail profiles were approximated as a bundle of equipotential thin-wire conductors, while computing the overall PULP of the entire rail as suggested in [11]. Subsequently, the thin-wire formulas in Appendix A have been applied, computing the equivalent radius that would be necessary in order to have the same PULP as for the actual rail. This radius was found to be equal to 76 mm for a standard UIC60 rail; with a typical height above the soil around 30–60 cm, rails largely satisfy the thin-wire approximation.

Once the PULP of the MTL are known, voltages and currents can be computed easily by means of the following expressions:

$$\mathbf{V}(z) = \mathbf{Z}_c \mathbf{T} [\mathbf{P}^+(z) \mathbf{I}_{m0}^+ + \mathbf{P}^-(z) \mathbf{I}_{m0}^-] \quad (2a)$$

$$\mathbf{I}(z) = \mathbf{T} [\mathbf{P}^+(z) \mathbf{I}_{m0}^+ - \mathbf{P}^-(z) \mathbf{I}_{m0}^-] \quad (2b)$$

where $\mathbf{P}^\pm(z) = \exp(\mp\gamma z)$ are the propagation matrices, \mathbf{Z}_c is the characteristic impedance matrix, γ is the diagonal matrix of modal propagation constants, and \mathbf{I}_{m0}^\pm are modal current excitation terms depending on boundary conditions at the line ends. Matrix \mathbf{T} and the propagation constants are related to the PULP matrices by means of the following eigenvalue expression:

$$(\mathbf{Y}\mathbf{Z})\mathbf{T} = \mathbf{T}\gamma^2. \quad (3)$$

A major issue in the analysis of railway systems is the modeling of power devices such as power supply substations, trains, overvoltage protections, and so on. Because these devices are electrically small, up to a few megahertz, they can all be modeled as lumped discontinuities. Although simplified equivalent circuits are available up to a few kilohertz for electric trains, characterizations covering an extended frequency range are not easily available. The reason for this lack of data is not only the fact that trains are tailor-made according to the customer's needs, but also due to practical difficulties in the experimental characterization of an active device that needs to be supplied under several thousands volts. Since this problem is common to any effort concerning railway systems modeling, this topic will not be addressed; this paper focuses on the way available models can be employed for the assessment of infrastructure impact.

Once equivalent representations are available for MTLs and lumped discontinuities, a railway system can be represented by means of an equivalent circuit that can be solved with well-established electric network analysis tools, e.g., the tableau method. In particular, the quantities we are interested in are the modal terms \mathbf{I}_{m0}^\pm for the line in front of the observer. Having access to their values, the current distribution along each conductor of this line can be computed by means of (2b).

The EM field radiated by a railway line can now be computed by means of antenna-theory methods. Wait's model [14], already used for the derivation of the PULP, can be applied, thus taking into account soil losses. The application of this model is very convenient, since it directly links the EM field in any point of the

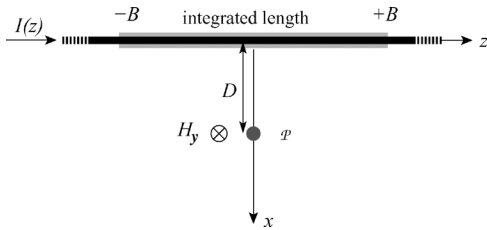


Fig. 3. Simplified configuration considered in order to check the accuracy of the magnetic field computed with finite integration bounds for an infinite line.

space with the current distribution. In its original formulation, the line was regarded as a single conductor. An extension to an MTL was proposed in [16], exploiting the modal decomposition applied in (2b). The magnetic field at position (x_o, y_o, z_o) can be computed as

$$H_y(x_o, y_o, z_o) = \sum_{i=1}^N \sum_{j=1}^N \Theta_{ik}(x_o, y_o) T_{ik} I_{m,k}(z_o) \quad (4)$$

where the current distribution $I_{m,k}(z)$ along the k th modal line is defined as

$$I_{m,k}(z) = I_{m0,k}^+ e^{-\gamma_k z} - I_{m0,k}^- e^{+\gamma_k z} \quad (5)$$

while the radiation matrix $\Theta(x, y)$ is given in Appendix B. The computation of the radiation matrix is relatively time-consuming because of the necessity to evaluate Sommerfeld integrals. A logarithmic approximation [17] can be applied to one of these integrals, yielding an analytical solution; for the remaining ones, rather than numerically integrating them, their kernel was approximated through Prony's method [18]. The result of this operation is the expansion of the kernels of Sommerfeld integrals into a complex exponential sum, such as

$$f(\lambda) \simeq \sum_{i=1}^N c_i e^{a_i \lambda} \quad (6)$$

which can be easily integrated analytically. The expansion parameters c_i and a_i are obtained through a nonlinear fitting procedure.

The only problem with Wait's model is that it assumes the line to be infinitely long. Since this is never the case, one must check when and how this model can be applied to finite lines. Let us consider an infinite line: one could rightfully claim that the main contribution to the magnetic field comes from a portion $2B$ of line centered just in front of the observer. In other words, there exists a B so that the contribution from the portion $[-\infty, -B] \cup [B, +\infty]$ is negligible; under such conditions, an infinite line behaves as if it were finite for the radiation estimate.

In order to check under which conditions this approximation can be invoked, let us consider a complex exponential current distribution in free space along the z -axis, as in Fig. 3. The magnetic field it excites can be computed by convolving the current distribution with the free-space Green's function; the absolute value of the resulting integrand function is mainly proportional to the function $1/\rho^3$ in the near-field. The error introduced by

this approximation is actually negligible, since the observer is in the very near-field of the radiator ($D \leq 10$ m, $f < 1$ MHz); this corresponds to a quasi-static configuration, even though a complex current distribution has been considered. For such a simple configuration, one can analytically compute the magnetic field at a distance D from the line (see Fig. 3), as excited by the entire infinite current distribution; in the same way, one can compute the contribution given by a limited portion of the current distribution, over a range $z \in [-B, +B]$. The definition of the integration efficiency η as in (7) allows us to assess the accuracy that can be attained by fixing a bound B

$$\eta[1/\rho^3] = \frac{\int_{-B}^{+B} dz/\rho^3}{\int_{-\infty}^{+\infty} dz/\rho^3} = \frac{B/D}{\sqrt{1 + (B/D)^2}}. \quad (7)$$

Although derived under strong approximations, expression (7) works remarkably well. By fixing an accuracy $\eta > 0.9$ (error < 1 dB), one gets $B/D > 3$; this rule of thumb has been checked by computing the magnetic field along an MTL through the numerical integration of Sommerfeld's model for an electric dipole above a lossy soil [19], limiting the integration to the interval $[-B, +B]$ given by (7) and comparing these results to Wait's infinite line model. The cross section of the line has been chosen to represent an actual railway line, with a length of 1 km: the results obtained just below the overhead conductors and 10 m away from them have proven that (7) is actually slightly conservative [6].

Practically, this rule of thumb means that an infinite line model can be applied to a finite one as long as the observer is at a distance B from any discontinuities. This also implies that the modeling tools presented here cannot be used for the computation of the magnetic field as measured in front of a train. This limitation is not only due to the use of an infinite line model, but also due to the fact that the presence of the train chassis would inevitably require a numerical approach. Nevertheless, this is not a limitation with respect to the target set here: even though the magnetic field is measured away from the train position, the tools introduced here can be effectively used for the estimation of the infrastructure impact. Actually, (7) yields $B > 30$ m for an observer 10 m away from the line: this distance is electrically small up to 1 MHz, so that the magnetic field is not expected to vary appreciably along it.

III. ON THE MODELING OF ACTUAL LINES

Before applying the modeling tools presented in Section II to actual railway lines, there are still some open issues. The paradigm of a uniform MTL introduced in the previous section can be regarded, at first, as not really fit to model a railway line (Fig. 4); the main points that could be raised are the presence of: 1) discontinuities provided by masts; 2) a rock ballast below the rails; and 3) short circuits between the overhead conductors.

The problem with the first point is that, should the masts have a nonnegligible effect, one would need to include them in the railway system description, by means of lumped circuits, every 50–70 m, thus increasing the system complexity. Numerical simulations of realistic mast structures using numerical electromagnetics code 2 (NEC2) (method of moments) have shown

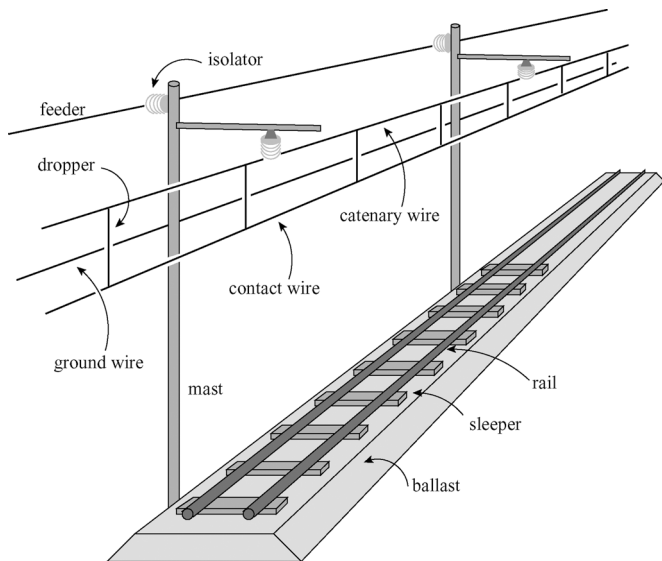


Fig. 4. Schematic representation of an actual railway line.

that they can be effectively modeled as $13\text{-}\mu\text{H}$ inductances up to 3 MHz [6]. Nevertheless, masts are always connected in series to overhead conductors by means of power isolators: since these latter ones basically behave as capacitances limited to a few picofarads, they dominate the overall impedance seen from the railway line, providing a very high impedance path. Simulations including masts and power isolators have shown no remarkable differences in the current distribution with respect to the case of a uniform structure, so that the presence of masts can be neglected.

Another point is the presence of a rock ballast. Other authors [20], [21] have presented results from the experimental estimation of the PULP of a railway line, showing that a rock ballast introduces equivalent conductances between the rails and the soil. Nevertheless, the effect of the rock ballast is expected to be mostly negligible over the frequency range investigated here; the argument that can be brought to this claim is that rock ballasts are made of low conductive rocks (mostly quartzite), which are not electrically connected, but rather interfilled with air. Usually this argument is regarded as insufficient due to the high humidity rates that can be attained during rainy weather. Nevertheless, the experimental results shown in Section IV have been obtained exactly with such conditions, thus suggesting the validity of this approximation.

The last argument is the presence of short circuits along the overhead conductors. The electrical distance between them is short enough to apply the idea of having distributed short circuits along the overhead conductors, rather than lumped ones. The advantage of this approach is that we can directly intervene on the PULP representation of the MTL; considering all the overhead conductors as equipotential implies that the catenary system inherently behaves as a single conductor. Equivalent PULP can then be derived for this equivalent representation [11] with just one equivalent overhead conductor. The resulting reduction in the catenary complexity implies a reduction of the computation time spent in solving the equivalent railway circuit and in the

computation of the radiation matrix Θ . With respect to this last point, the equivalent overhead conductor lays in the mechanical center of the original overhead bundle. The idea of an equivalent single-wire catenary also provides an easy way to check the importance of nonuniformities in the overhead line, namely a camber. Its importance can be assessed by computing the equivalent PULP for the cross section in the two extreme positions of the camber of a real-life line: a three-wire overhead line is considered here with heights $[5, 5.3, 5.6]$ m and $[5, 5.3, 6.3]$ m. The resulting PULP for the two configurations differ less than 5%, so that the camber can actually be neglected.

Having settled these issues, before using these tools for assessing the infrastructure impact, it is profitable to apply TLT results in order to check whether the negligible-resonances condition stated in the standard EN 50121 holds. This condition requires that the energy associated with backward-traveling modes must be negligible with respect to the forward-traveling ones. This problem is actually dominated by the less attenuated mode; hence, it suffices to analyze it by defining a sort of reflection coefficient Γ_m whose modulus depends on the line length as

$$\Gamma_m \leq e^{-2\alpha_0 \mathcal{L}} \quad (8)$$

where α_0 is the attenuation constant for the less attenuated mode. This result could be regarded as too conservative. Anyway, applying it to a three-conductor line (i.e., by simplifying an actual railway line by reducing equipotential conductors), the dominant mode is indeed the one describing the differential propagation between the catenary and the rails, which coincides with the least attenuated. Since the propagation mainly follows this pattern, condition (8) is expected to be representative of the actual propagation.

Equation (8) has then been used in order to compute the minimum length required to have negligible reflections, taking $\Gamma_m < 0.3$ (-10 dB) as a reasonable value. The results of this operation are shown in Fig. 5, compared to the 3-km length suggested by the standard: it is interesting to notice that below 1 MHz, the required length is far greater than 3 km, and it can attain very large values in the lower frequency range. In other words, these structures are not as lossy as assumed by the standard; therefore, the potential excitation of resonances is underestimated by the standard. A further condition worsens this scenario: the spectrum of conducted EMI generated by switched-mode devices is usually richer below 1 MHz (depending on the modulation scheme of the switched-mode converter), so that there is a nonnegligible possibility that the indirect contribution from conducted EMI be amplified by resonances.

IV. EXPERIMENTAL VALIDATION

The model introduced here has been validated through experimental tests performed on actual railway lines. The basic configuration of the setup is shown in Fig. 6. The aim is to measure the lateral component of the magnetic field as excited by a function generator connected to the line under test (LUT), between the overhead line (through an isolating hooked stick connected to a metallic wire) and the two rails short-circuited together, while at

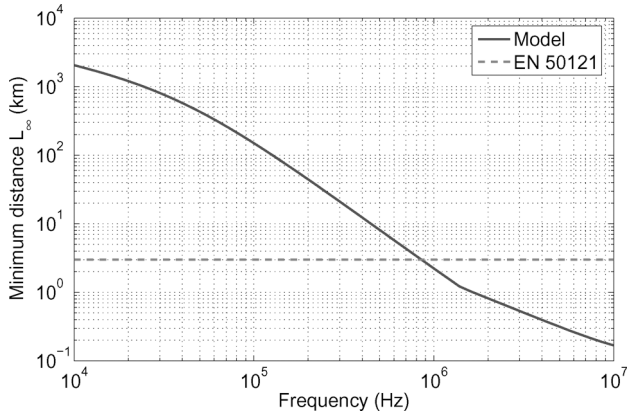


Fig. 5. Simulation results for the minimum length \mathcal{L}_∞ required to regard a railway line as resonance-free.

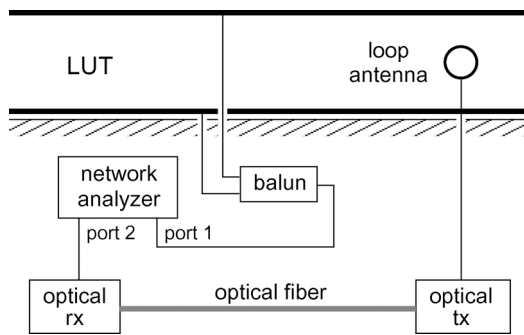
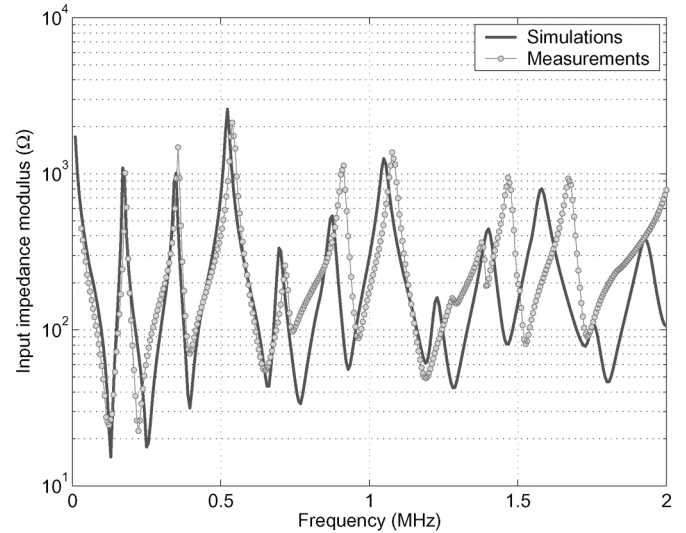


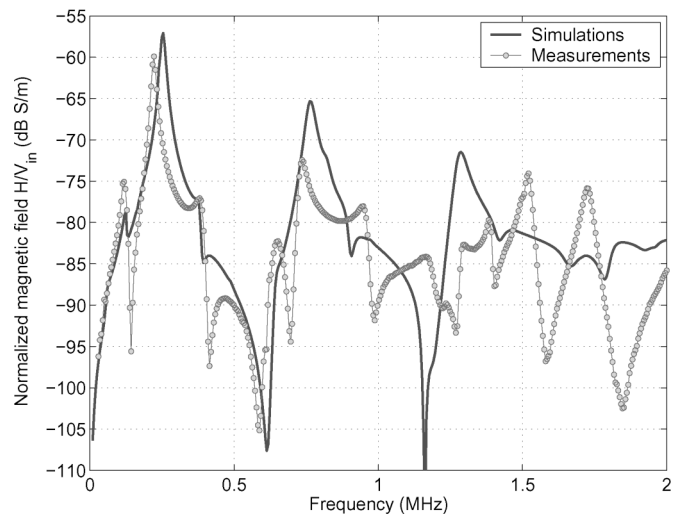
Fig. 6. Measurement setup for the experimental validation on an actual railway line.

the same time, the input impedance of the line, as seen through the output port of the sine-wave generator, is measured, in order to have a trace of the frequency dependence of propagation along the LUT. The use of a network analyzer (NA), although requiring due attention in a high-voltage environment, allows a noise rejection far greater than with asynchronous schemes, e.g., with a spectrum analyzer (SA), while providing a greater sensitivity. One problem with this setup is the need to link the loop antenna and the NA. The simplest solution would be the use of a coaxial cable running along the LUT, but ultimately leading to perturbations in the magnetic field measurements. This problem was avoided by using an optical fiber link. A balun based on a wide-frequency transformer (3-dB passband over 1 kHz–30 MHz) was employed for the excitation of the LUT in order to ensure an ideally differential excitation and a galvanic isolation between the LUT and the NA. The need for a differential excitation is justified by its easier modeling, thus ensuring a more meaningful comparison between experimental and theoretical results.

Several tests were carried out, mainly on two sites: at the CEF and at a facility at Alstom Transport, both in Valenciennes, France. Unfortunately, strong constraints (of commercial and safety nature, time schedule, and so on) make tests on commercial lines, rather than on facilities, very unlikely. Therefore, no experimental validation has been carried out on lines longer than 3 km. Moreover, even the two aforementioned facilities



(a)



(b)

Fig. 7. Experimental results for (a) the input impedance and (b) the magnetic field measured on an Alstom Transport site.

were seldom available, and if available, then for very short sessions; hence, just a small number of tests were performed.

The results presented here refer to the Alstom site, which is 835 m long, with a four-wire catenary and a rock ballast about 30 cm thick; the LUT was electrically disconnected from any power source such as power supply substations. Some results from the validation are shown in Fig. 7; the NA was connected to the line 285 m away from its left end, while the antenna stood at 240 m, 5 m away from the line axis, 1.4 m above the soil. Both the line ends were open-circuited.

The agreement between theory and measurements is satisfactory up to 700 kHz, with errors in the magnetic field computation limited to less than 5 dB. The results on the input impedance Z_{in} actually show that the propagation is also well modeled over the range 1–1.2 MHz; therefore, the current distribution is expected to be properly identified. Nevertheless, the trend in the magnetic field is not correctly predicted in this case: this means

that the disagreement over this frequency range was likely due to limitations in the validity of the radiation formulas. A closer look at the way the disagreement evolves in Z_{in} shows that it is likely due, at least, to an increasing error in the evaluation of propagation constants, as pointed out by the increasing shift in the maxima and minima. This is likely due to our having neglected the dielectric nature of the ballast, as to the fact that the length of the line is just known to a 2% degree of accuracy.

V. ASSESSMENT OF THE INFRASTRUCTURE IMPACT

In order to model radiated emission results, equivalent models are needed for the train too. Actually, the very idea of modeling a train in the frequency domain may look incongruous with the fact that switched-mode regulators have a strong nonlinear behavior. Nevertheless, such an approach is valid in a steady-state analysis, as in this context. In particular, nonlinear circuits performing modulation/regulation can be analyzed by means of Fourier series [5], [22], assessing the spectrum of the conducted emissions they generate, according to the modulation scheme they implement. The resulting spectrum is almost independent of the load characteristics, but for the power factor seen by the switched-mode circuit [5], even above the 1-MHz region. In particular, a switched-mode converter can be represented, for the sake of conducted EMI, as an independent voltage generator in series with an impedance Z_t . While the generator accounts for the conducted EMI spectrum, the impedance Z_t represents all the remaining linear parts of the converter, such as wiring, EMI filters, and so on [23]–[25]. The resulting equivalent circuit is thus valid just as a small-signal model, implying the linearization of the nonlinear systems in a steady-state configuration.

Supposing to have such an equivalent model, we could compute the magnetic field that would be measured by an observer. By performing this operation for the actual site and for the case where the train is connected to an infinite uniform line (the ideal site envisaged by the standard), the infrastructure impact $W(f)$ could be defined as

$$W(f) = \frac{|H_a(f)|}{|H_i(f)|} \quad (9)$$

where $H_a(f)$ and $H_i(f)$ are the magnetic fields for, respectively, the actual and the ideal lines, as measured from the observer position. The function $W(f)$ therefore assesses how the magnetic field spectrum is distorted by the fact of having carried out the tests along a nonideal railway line. Values greater than 1 indicates that the actual site resonances are indeed worsening the indirect radiated EMI of the train, with the risk of regarding it as noncompliant. Unfortunately, to the best of our knowledge, equivalent circuits for conducted EMI are not available for trains. However, thanks to the near-independence of the equivalent circuit from its loading impedance [5], $W(f)$ can be assessed by introducing the site transfer function $\beta(f)$

$$H(f) = \beta(f)I_{in}(f) \quad (10)$$

where I_{in} is the current injected by the train through the pantograph (Fig. 8). The infrastructure impact can now be expressed

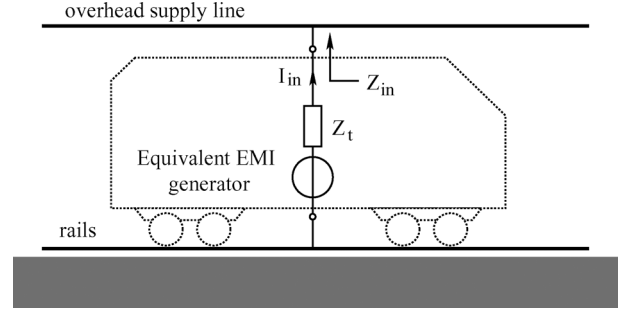


Fig. 8. Equivalent circuit representation used in the assessment of the infrastructure impact $W(f)$.

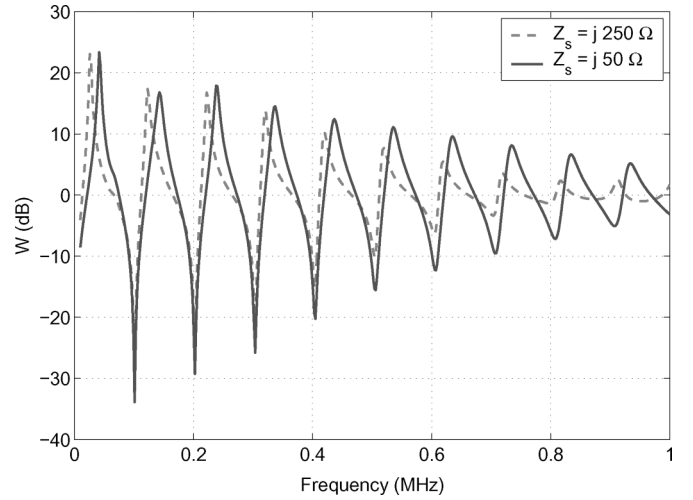


Fig. 9. Distortion factors showing the infrastructure impact for an open-circuited line 3 km long, with the train in the middle of the track. The magnetic field has been computed 10 m away from the line, 2 m high above the soil, and 50 m at the right of the train. Two equivalent internal train impedances have been considered.

as

$$W(f) = \frac{|H_a(f)|}{|H_i(f)|} = \frac{|\beta_a(f)|}{|\beta_i(f)|} \frac{|Z_t(f) + Z_{in,i}(f)|}{|Z_t(f) + Z_{in,a}(f)|} \quad (11)$$

where $Z_{in}(f)$ is the input impedance of the track, as seen from the train between the catenary and the rails. This kind of approach has the advantage of not requiring the knowledge of the equivalent voltage generator, but just of its internal impedance, by invoking the low sensitivity to the site configuration of the equivalent EMI generator. It is important to recall that the train impedance Z_t is independent of the input impedance of the line $Z_{in}(f)$, since it is just related to linear circuits.

An example of results obtained with this procedure is shown in Fig. 9, where the actual site is a uniform track 3 km long, with open-circuited ends, and the train placed in the middle of the track. The internal impedance Z_t of the train has been assumed to be inductive, considering the two values $50j \Omega$ and $250j \Omega$. These values are not meant to be representative of an actual train; they are just considered as an example for discussing the infrastructure impact $W(f)$. As a matter of fact, Z_t can be expected to be strongly dependent on frequency, much in the

same way as for the high-frequency behavior of a low-frequency transformer.

The results in Fig. 9 are quite self-explaining; indeed, resonances can distort the results of the radiated emissions test, in two respects: the most evident effect is the increase in the maxima, which can easily exceed 10 dB. But this is not the only effect, since whenever important conducted EMI harmonics occur at the same frequency as a minimum in the transfer function, their importance can be underestimated. This eventuality, although unlikely, represents a treat to the effectiveness of the standard, since noncompliant trains could not be identified as such, if tested on certain railway sites.

VI. EXPERIMENTAL CHARACTERIZATION OF A RAILWAY LINE

Unfortunately, three obstacles impede the use of a predictive model: 1) the literature is very poor about high-frequency equivalent models for power devices, which may be required to be characterized under a high-voltage supply; 2) not even the site owner is able to provide an accurate description of the test site, not only from a geometrical point of view, but also regarding the presence of partially hidden power devices such as for over-voltage protection; 3) because of the very feeble propagation attenuation in the lower frequency range, portions of the site physically very distant (several 10 km) from the TUT may have a nonnegligible effect on the overall infrastructure impact; since this would require a very large extension of the site to be modeled, the work required to describe it would be hardly justified. These three points are a formidable challenge to any actual modeling attempt. Therefore, predictive models are more likely to be useful as reference tools to understand the phenomena involved in the excitation of radiated emissions, or during design sessions.

On the other hand, a more feasible approach is proposed here. Rather than pursuing a predictive simulation, an equivalent model of the site can be derived from experimental measurements with no *a priori* information. The first step to be undertaken is to identify a portion of line clear of any significant discontinuities that will be referred to as the reference line. Since the tests are to be carried out in a steady-state configuration, all the power devices connected to the remaining portion of the test site can be described through Thévenin-like equivalent circuits. Hence, because the rest of the elements in a test site are linear, a more general equivalent circuit can be defined representing the entire test site outside the reference line where the TUT lies by means of two equivalent circuits (Fig. 10). Once these two circuits are available, the entire actual system can be accurately simulated; on the other hand, the response of the ideal site can be easily estimated by substituting these two equivalents with the characteristic impedance matrix of the reference line, thus simulating an infinite line.

In order to estimate the two equivalents, we here propose a procedure based on magnetic field measurements by defining the inverse problem

$$\mathbf{H}_m = \mathbf{f}(\mathbf{p}) \quad (12)$$

where \mathbf{p} is a vector containing the unknown parameters defining the equivalent circuits, \mathbf{H}_m is a vector of magnetic

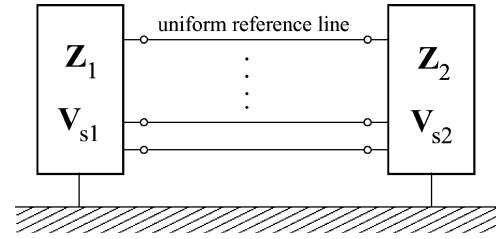


Fig. 10. Equivalent site representation sought here, based on the identification of a reference uniform line.

field measurements (amplitude-only data from the SA), and $\mathbf{f}(\cdot)$ is a function relating the equivalent description of the site (through the uniform line and the set of parameters \mathbf{p}) to the theoretical magnetic field. This last operation employs the previously introduced model in a predictive way. The equals sign in (12) is to be taken in a weak sense, as we have chosen to look for a least square solution.

The proposed approach consists of two steps: 1) collecting the data and 2) solving an optimization problem through predictive simulations. The first point is accomplished by exploiting the ambient noise of the site; as a matter of fact, this background magnetic field, mostly excited by conducted EMI propagating along the supply line and generated by substations and other trains, contains information about the electrical configuration of the entire site. The second step deals with an optimization problem aiming at solving (12) through the minimization of the error function $e(\mathbf{p})$

$$e(\mathbf{p}) = \|\mathbf{H}_m - \mathbf{f}(\mathbf{p})\|_2. \quad (13)$$

The feasibility of this latter task strongly depends on the amount and quality of available experimental data. Conversely, as for many inverse problems, the solution of this problem is unstable, due to its ill-posed nature: indeed, there exists a number of electrical configurations that can provide very similar results. During the “inversion,” this leads to a strong sensitivity of the equivalent parameters with respect to the magnetic field measurements. Two actions are to be taken in order to reduce this instability: by increasing the amount of uncorrelated magnetic field measurements, we get more information on the electrical configuration we are looking for, whereas by introducing *a priori* information, the problem is regularized, i.e., its sensitivity is reduced.

In order to actually collect meaningful information, the magnetic field samples should be measured at least at a distance of $\lambda/10$ from each other; satisfying this requirement implies that the length of the reference line should be proportional to the maximum wavelength, corresponding to the minimum frequency of interest. Considering a few tens kilohertz, this would mean to consider several tens kilometers, which would require the antenna and the SA (together with their energy supply) to be moved along this distance. Practical aspects would limit the reference line to a few hundred meters: therefore, samples in the lower frequency range will be quite similar, thus with a limited amount of information. More information can be obtained by locally modifying the electrical configuration of the test site. By adding lumped loads at the ends of the reference line, the

measured magnetic field will be modified too; nevertheless, it will still depend on the rest of the site, i.e., the configuration we are interested in, while bringing additional data. Practically, this idea would require the use of a high-voltage decoupling capacitor inserted between the load and the overhead line (by means of an isolating hooked stick), thus allowing the use of low-voltage loads. High-capacitance power isolators could be used as decoupling capacitors. The aim here is to introduce a perturbation that will just be seen from the EMI viewpoint, while the power electronics will still see the same low-frequency loads, so as to ensure the time invariance of the system.

On the other hand, the inverse problem can be regularized by reducing the degrees of freedom. For instance, passivity should be enforced by requiring the impedance matrices \mathbf{Z} to have a positively definite real part. Furthermore, symmetry can be exploited, e.g., one can rightfully assume the two rails to be electrically symmetrical. Finally, the number of unknowns can be decreased by reducing the overhead line to a single conductor. The simplest solution to the inverse problem follows a trial-and-error scheme. At each run, the vector \mathbf{p} is randomly generated as a guess value: these parameters identify a certain electrical configuration of the site. By applying the previous model in a predictive way, the magnetic field is estimated at the same locations where it has been actually measured. This first phase is usually referred to as direct solution. This operation is carried out for a certain number of runs, then a minimum search method is applied, keeping track of the partial solution giving the lowest value for the error $e(\mathbf{p})$. The random approach allows a rough inspection of the solution space defined by \mathbf{p} , which is characterized by widely variable parameters, e.g., impedance can range from a short circuit to an open one, due to the resonant nature of the system. This approach is far from optimal, and its poor performance are worsened by the fact that there is no assurance to find the global minimum. Actually, the aim here was just to prove the feasibility of this approach, while actual implementations for industrial applications will require further investigations in order to effectively solve the inverse problem with an acceptable confidence margin. Furthermore, we had no possibility to carry out experimental validations, which justifies the all-numerical investigation.

A numerical feasibility test for this approach has been carried out by considering the railway line in Fig. 11(a). Five magnetic field samples have been computed along the 700-m reference line. In order to increase the amount of data, nine load configurations have been applied to the ends of the reference line, considering three loads: an open circuit, and a 50- and a 300- Ω resistance, making a grand total of 45 spectra. The two equivalent circuits have been estimated just up to 200 kHz, since at higher frequencies, the inverse problem is expected to be less critical. From this equivalent representation, the magnetic field has been computed for the two configurations shown in Fig. 11(b), where the TUT is represented as a Thévenin-like equivalent. The results of this operation are shown in Fig. 12, as obtained from 50 runs, compared with the results obtained by simulating the original description in Fig. 11(a). Indeed, the trend in the spectra is fairly well identified, even though there are important disagreements: in particular, as expected, in the lower frequency

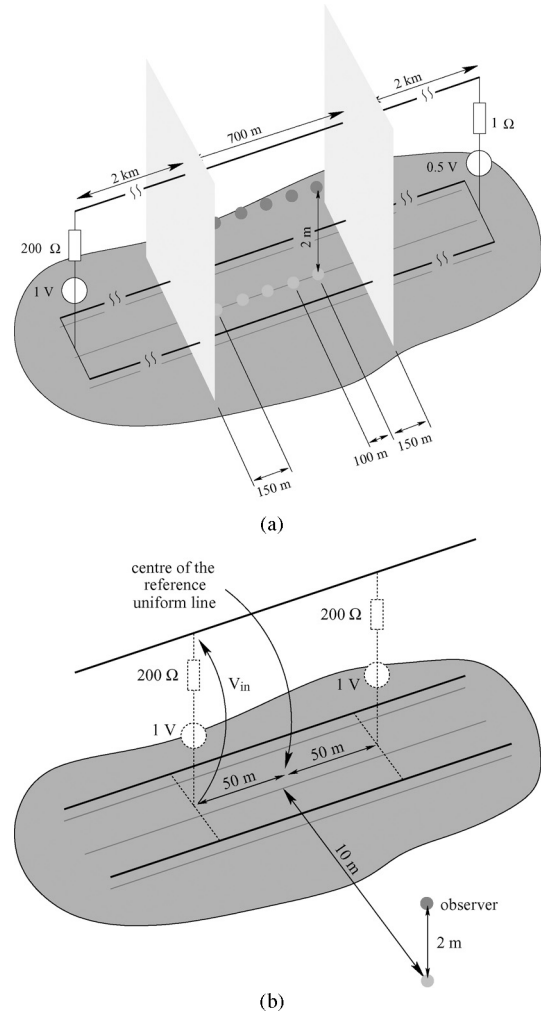


Fig. 11. Feasibility test for the experimental site characterization. (a) Three-wire line considered for the numerical validation of the site characterization approach. The reference uniform line as defined by two reference planes, together with the five positions where the magnetic field is measured. (b) Two configurations tested for validating the site characterization.

range. Beside the validation of the characterization procedure, the infrastructure impact has been pointed out by substituting the two equivalent representations at the uniform line ends with the characteristic impedance matrix \mathbf{Z}_c ; the magnetic field computed for this configuration is also shown in Fig. 12. Therefore, a procedure as the one described here would allow the manufacturer to characterize a site before actually testing the train, providing a tool for assessing the impact of the infrastructure.

Nevertheless, in order to make an industrial tool out of this idea, one should find a way to ensure, up to a certain degree, the convergence of the optimization routine toward the global minimum. A likely way to improve it is to apply a simulating annealing approach, which generalizes the idea of a random search for the global minimum, but gradually reducing its range of variability, thus providing a sort of convergence, even without ensuring the ability to find the global minimum. Besides, a better optimization routine would also relax the need for information, and in particular, it could lead to a measurement routine without the need to apply load pairs; this would make

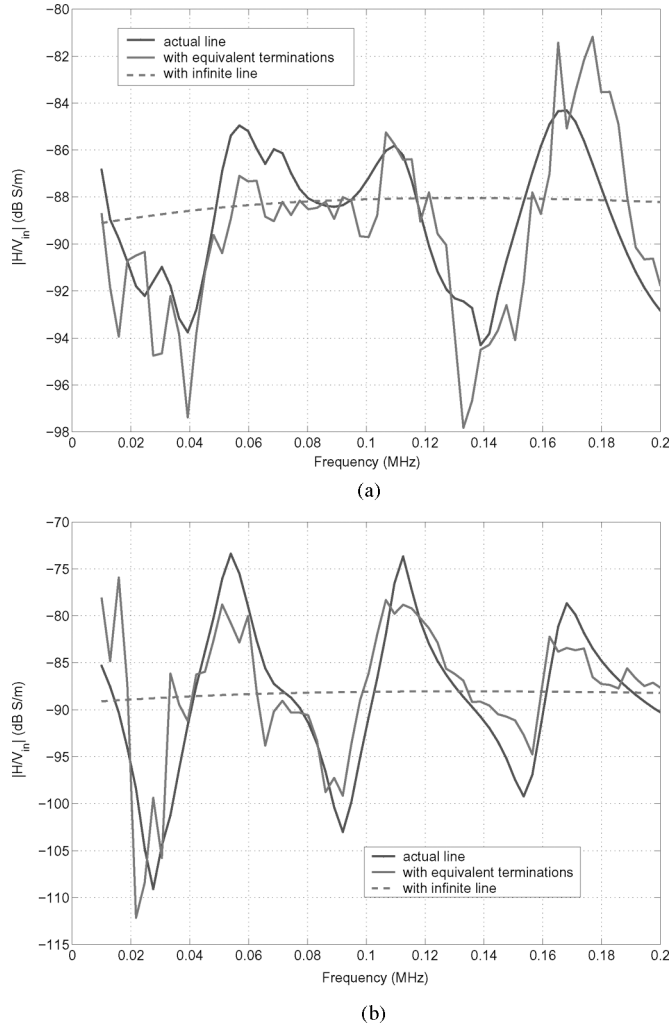


Fig. 12. Results of the numerical validation for the experimental site characterization, showing the magnetic field computed for the system in Fig. 11(a) and the one computed by using its equivalent characterization. Two positions are considered for the train. (a) Left side of the uniform line. (b) Right side. The magnetic field that would have been obtained with an infinite line is also shown.

an even stronger case for the use of this characterization technique. This approach indirectly implies the time invariance of the site, whose equivalent electrical configuration is not supposed to vary significantly between the site characterization and the testing of the train. Such hypothesis could prove not to hold when considering sites with trains moving or changing the loading of power supply substations.

VII. CONCLUSION

In this paper, we have addressed the problem of modeling electric railway lines in order to assess the infrastructure impact in testing radiated emissions of rolling stock. In the first part, we proposed the use of a theoretical description of the test site where the train is to be tested. By simulating the response of the actual site and comparing it with the ideal resonance-free site envisaged by the standard EN 50121, one can distinguish between excessive magnetic field values due to the train or rather due to resonances of the infrastructure. The model described

here has shown to be accurate enough when applied to actual railway lines up to 700 kHz, even with the introduction of approximations for the treatment of nonidealities of railway lines (overhead line reduction, ballast, cambers, etc.).

This model has then been used to check the accuracy of the negligible-resonance hypothesis stated in the standard, proving its inaccuracy and the subsequent underestimation of infrastructure resonances, due to the overestimation of propagation attenuation. This, together with the difficulties in getting a fair description of the test site and of related power devices, has pointed out the strong limitations any modeling efforts are bound to encounter. For these reasons, we have finally proposed an alternative experimental characterization based on magnetic field measurements with no *a priori* information of the actual site configuration. The feasibility of this approach has been demonstrated through a numerical study, emphasizing the limitations due to the numerical solution of this inverse problem. Although further investigations have to be carried out, an improved version of this approach currently seems to be the only practical way of characterizing a railway site, and subsequently of assessing the impact of its configuration in radiated emissions tests.

APPENDIX

A. PULP for an MTL Above a Lossy Soil

The following expressions refer to results presented in [13]. For the sake of simplicity, the notation is simplified here, though referring to the quasi-static solution obtained under a logarithmic approximation [17]

$$\mathbf{A} = (\mathbf{\Lambda} + 2\mathbf{S}_2^h)^{-1} (\mathbf{\Lambda} + 2\mathbf{S}_1^h) \quad (14)$$

$$\mathbf{Z}_e = \frac{j\omega\mu_0}{2\pi} \mathbf{\Lambda} \quad (15)$$

$$\mathbf{Y}_e = j\omega\epsilon_0 2\pi \mathbf{\Lambda}^{-1} \quad (16)$$

$$\mathbf{Z}_g = \frac{j\omega\mu_0}{\pi} (\mathbf{S}_1^h - \mathbf{S}_2^0 \mathbf{A}) \quad (17)$$

$$\mathbf{Y}_g = j\omega\epsilon_0 \pi (\mathbf{S}_2^h - \mathbf{S}_2^0)^{-1} \quad (18)$$

The quasi-static approximation of the remaining matrices is given by

$$\Lambda_{ik} \simeq \frac{1}{2} \ln \left[\frac{h_+^2 + d^2}{h_-^2 + d^2} \right] \quad (19)$$

$$S_{1,ik}^h \simeq \frac{1}{4} \ln \left[\frac{(h_+ + c_1)^2 + d^2}{h_+^2 + d^2} \right] \quad (20)$$

$$S_{2,ik}^h \simeq \frac{1}{2(1 + \tilde{\epsilon})} \ln \left[\frac{(h_+ + c_2)^2 + d^2}{h_+^2 + d^2} \right] \quad (21)$$

$$S_{1,ik}^0 \simeq \frac{1}{4} \ln \left[\frac{(h_i + c_1)^2 + d^2}{h_i^2 + d^2} \right] \quad (22)$$

$$S_{2,ik}^0 \simeq \frac{1}{2(1 + \tilde{\epsilon})} \ln \left[\frac{(h_i + c_2)^2 + d^2}{h_i^2 + d^2} \right] \quad (23)$$

where $h_{\pm} = h_k \pm h_i$, $d = d_k + r_k - d_i$, and with $\beta = \gamma_0(\tilde{\epsilon} - 1)$, $c_1 = 2/\beta$, $c_2 = (1 + \tilde{\epsilon})/\beta$, $\gamma_0 = jk_0$ being the free-space propagation constant.

B. Magnetic Field Near an MTL Above a Lossy Soil

These results have been originally presented in [16]

$$\Theta_{ik} = \frac{1}{\pi} (-\Upsilon_{ik} + k_0^2 \mathcal{J}_{1,ik} + \gamma_k^2 \mathcal{J}_{2,ik} + \mathcal{J}_{3,ik}) \quad (24)$$

with

$$\Upsilon_{ik} = \frac{\Gamma_k}{2} \left[\frac{x_o + h_i}{\rho_{+,i}} K_1(\Gamma_k \rho_{+,i}) - \frac{x_o - h_i}{\rho_{-,i}} K_1(\Gamma_k \rho_{-,i}) \right] \quad (25a)$$

$$\mathcal{J}_{1,ik} = \int_0^\infty \frac{\phi_1}{u_{0,k}} \cos[\lambda(y_o - d_i)] d\lambda \quad (25b)$$

$$\mathcal{J}_{2,ik} = \int_0^\infty \frac{\phi_\varepsilon}{u_{0,k}} \phi_\varepsilon \cos[\lambda(y_o - d_i)] d\lambda \quad (25c)$$

$$\mathcal{J}_{3,ik} = \int_0^\infty \lambda^2 \frac{\phi_1}{u_{0,k}} \cos[\lambda(y_o - d_i)] d\lambda \quad (25d)$$

where $K_1(\cdot)$ is the modified Bessel function of the second type, first-order, $\Gamma_k^2 = \gamma_0^2 - \gamma_k^2$, and the kernels ϕ are to be read as $\phi(\gamma_k, x_o + h_i, \lambda)$, having defined

$$\phi_\chi(\gamma_k, x, \lambda) = \frac{e^{-u_{0,k} x}}{\chi u_{0,k} + u_{g,k}} \quad (26)$$

with $u_{0,k}^2 = \lambda^2 - \gamma_k^2 + \gamma_0^2$, $u_{g,k}^2 = \lambda^2 - \gamma_k^2 + \tilde{\varepsilon} \gamma_0^2$, and $\rho_{\pm,i}^2 = (x_o \pm h_i)^2 + (y_o - d_i)^2$.

ACKNOWLEDGMENT

This work was carried out during the Ph.D. thesis of the first author under an agreement between Alstom Transport (St. Ouen, France), CEF (Valenciennes, France), the Politecnico di Torino (Turin, Italy), and IEMN/TELICE.

REFERENCES

- [1] T. Konefal, D. A. J. Pearce, C. A. Marshman, and L. M. McCormack, *Potential Electromagnetic Interference to Radio Services From Railways*, Radiocommun. Agency, 1st issue, York EMC Services Ltd., Univ. York, York, U.K., Final Rep. AY4110.
- [2] *Railway Applications—Electromagnetic Compatibility*, CENELEC Standard EN 50121, 2006.
- [3] R. J. Hill, "Electric railway traction: Part 3. Traction power supplies," *Inst. Electr. Eng. Power Eng. J.*, vol. 8, no. 6, pp. 275–286, Dec. 1994.
- [4] P. Chapas, *Traction Ferroviaire*. Levallois-Perret Cedex, France: Alstom Transport, Sep. 1999.
- [5] L. Tihanyi, *Electromagnetic Compatibility in Power Electronics*. Piscataway, NJ: IEEE Press, 1995.
- [6] A. Cozza, "Railways EMC: Assessment of infrastructure impact," Ph.D. dissertation, Université des Sciences et Technologies de Lille, Lille, France, Jun. 22, 2005. (Available at request from the authors)
- [7] E. F. Vance, *Coupling to Shielded Cables*. New York: Wiley, 1977.
- [8] F. Kuester, D. C. Chang, and R. G. Olsen, "Modal theory of long horizontal wire structures above the Earth. 1. Excitation," *Radio Sci.*, vol. 13, no. 4, pp. 556–557, Jul./Aug. 1978.
- [9] R. M. Sorbello, R. W. P. King, K. M. Lee, L. C. Shen, and T. T. Wu, "The horizontal-wire antenna over a dissipative half-space: Generalized formula and measurements," *IEEE Trans. Antennas Propag.*, vol. AP-25, no. 6, pp. 850–854, Nov. 1977.
- [10] P. Degauque, G. Courbet, and M. Heddebaut, "Propagation along a line parallel to the ground surface: Comparison between the exact solution and the quasi-TEM approximation," *IEEE Trans. Electromagn. Compat.*, vol. EMC-25, no. 4, pp. 422–427, Nov. 1983.
- [11] C. R. Paul, *Analysis of Multiconductor Transmission Lines*. New York: Wiley, 1994.
- [12] J. R. Carson, "Wave propagation in overhead wires with ground return," *Bell Syst. Tech. J.*, vol. 5, pp. 539–554, 1926.
- [13] M. D'Amore and M. S. Sarto, "Simulation models of a dissipative transmission line above a lossy ground for a wide frequency range—Part II: Multiconductor configuration," *IEEE Trans. Electromagn. Compat.*, vol. 38, no. 2, pp. 139–149, May 1996.
- [14] J. R. Wait, "Theory of wave propagation along a thin-wire parallel to an interface," *Radio Sci.*, vol. 7, no. 6, pp. 675–679, Jun. 1972.
- [15] G. E. Bridges and L. Shafai, "Validity of the thin-wire approximation of conductors near a material half-space," in *Antennas Propag. Soc. Int. Symp., AP-S Dig.*, Jun. 26–30, 1989, pp. 232–235.
- [16] M. D'Amore, M. S. Sarto, and A. Scarlatti, "Theoretical analysis of radiated emission from modal currents in multiconductor transmission lines above a lossy ground," in *Proc. IEEE Int. Symp. Electromagn. Compat.*, Aug. 21–25, 2000, vol. 2, pp. 729–734.
- [17] P. Pettersson, "Image representation of propagation of transients on overhead transmission lines," presented at the Cigré Symp., Lausanne, Switzerland, Oct. 1993, Paper 200-08.
- [18] S. L. Marple, *Digital Spectral Analysis: With Applications*. Englewood Cliffs, NJ: Prentice-Hall, 1986.
- [19] J. R. Wait, *Electromagnetic Wave Theory*. New York: Harper & Row, 1985.
- [20] R. J. Hill and D. C. Carpenter, "Rail track distributed transmission line impedance and admittance: Theoretical modeling and experimental results," *IEEE Trans. Veh. Technol.*, vol. 42, no. 2, pp. 225–241, May 1993.
- [21] A. Mariscotti and P. Pozzobon, "Synthesis of line impedance expressions for railway traction systems," *IEEE Trans. Veh. Technol.*, vol. 52, no. 2, pp. 420–430, Mar. 2003.
- [22] J. A. Taufiq and J. Xiaoping, "Fast accurate computation of the DC-side harmonics in a traction VSI drive," *Proc. Inst. Electr. Eng.*, vol. 136, no. 4, pp. 176–187, Jul. 1989.
- [23] R. J. Hill, "Electric railway traction: Part 6. Electromagnetic compatibility—Disturbance sources and equipment susceptibility," *Inst. Electr. Eng. Power Eng. J.*, vol. 11, no. 1, pp. 31–39, Feb. 1997.
- [24] J. Shen, J. A. Taufiq, and A. D. Mansell, "Analytical solution to harmonic characteristics of traction PWM converters," *Inst. Electr. Eng. Proc. Electr. Power Appl.*, vol. 144, no. 2, pp. 158–168, Mar. 1997.
- [25] X. Pei, K. Zhang, Y. Kang, and J. Chen, "Analytical estimation of common mode conducted EMI in PWM inverter," in *Proc. 26th Annu. Int. Telecommun. Energy Conf. (INTELEC 2004)*, Sep. 19–23, pp. 569–574.



Andrea Cozza (S'02–M'05) received the Laurea degree (*summa cum laude*) in electronic engineering from the Politecnico di Torino, Turin, Italy, in 2001, and the Ph.D. degree in electronic engineering from the Politecnico di Torino and the University of Lille, Lille, France, in 2005.

In 2007, he joined the Electromagnetics Research Department, L'École Supérieure d'Électricité (SUP-ELEC), Gif sur Yvette, France, as a Researcher and an Assistant Professor. His current research interests include modeling of transmission lines, near-field measurement techniques, reverberation chambers, electromagnetic dosimetry, and applications of time-reversal to electromagnetics.



Bernard Démoulin was born in Denain, France, on November 7, 1946. He received the M.S. and Ph.D. degrees from the Université de Sciences et Technologies de Lille, Villeneuve d'Ascq Cedex, France, in 1971 and 1973, respectively.

He is currently a Professor at the Université de Sciences et Technologies de Lille, where he works with the Telecommunication, Interferences and Electromagnetic Compatibility (TELICE) Group, Institut d'Électronique, de Microélectronique et de Nanotechnologie (IEMN) Laboratory. His current research interests include electromagnetic compatibility measurements especially in mode-stirred reverberation chambers and electromagnetic coupling computation throughout multiple-wire cables, as well as the characterization of integrated circuits in terms of susceptibility.

Prof. Démoulin is a Senior Member of the French Electrical Engineering Society (SEE) and a correspondent of the International Scientific Radio Union (URSI).